MTL TR 91-25



# FAILURE ANALYSIS OF THE APACHE MIXER PIVOT SUPPORT

VICTOR K. CHAMPAGNE, Jr., GARY WECHSLER, and
MARC S. PEPI
U.S. ARMY MATERIALS TECHNOLOGY LABORATORY
MATERIALS TESTING AND EVALUATION BRANCH

KIRIT J. BHANSALI
U.S. ARMY AVIATION SYSTEMS COMMAND, ST. LOUIS, MO
ENGINEERING DIRECTORATE, STRUCTURAL AND MATERIALS DIVISION

July 1991



Approved for public release; distribution unlimited.

*Original contains color plates: All DTIC reproductions will be in black and white*



US ARMY
LABORATORY COMMAND
MATERIALS TECHNOLOGY LABORATORY

U.S. ARMY MATERIALS TECHNOLOGY LABORATORY
Watertown, Massachusetts 02172-0001

The findings in this report are not to be construed as an official Department of the Army position, unless so designated by other authorized documents.

Mention of any trade names or manufacturers in this report shall not be construed as advertising nor as an official indorsement or approval of such products or companies by the United States Government.

DISPOSITION INSTRUCTIONS

Destroy this report when it is no longer needed.
Do not return it to the originator

UNCLASSIFIED

SECURITY CLASSIFICATION OF THIS PAGE *(When Data Entered)*

| REPORT DOCUMENTATION PAGE | | READ INSTRUCTIONS BEFORE COMPLETING FORM |
|---|---|---|
| 1. REPORT NUMBER<br>MTL TR 91-25 | 2. GOVT ACCESSION NO. | 3. RECIPIENT'S CATALOG NUMBER |
| 4. TITLE *(and Subtitle)*<br>FAILURE ANALYSIS OF THE APACHE MIXER PIVOT SUPPORT | | 5. TYPE OF REPORT & PERIOD COVERED<br>Final Report<br>6. PERFORMING ORG. REPORT NUMBER |
| 7. AUTHOR*(s)*<br>Victor K. Champagne, Jr., Gary Wechsler, Marc S. Pepi, and Kirit J. Bhansali* | | 8. CONTRACT OR GRANT NUMBER*(s)* |
| 9. PERFORMING ORGANIZATION NAME AND ADDRESS<br>U.S. Army Materials Technology Laboratory<br>Watertown, Massachusetts 02172-0001<br>SLCMT-MRM | | 10. PROGRAM ELEMENT, PROJECT, TASK AREA & WORK UNIT NUMBERS |
| 11. CONTROLLING OFFICE NAME AND ADDRESS<br>U.S. Army Laboratory Command<br>2800 Powder Mill Road<br>Adelphi, Maryland 20783-1145 | | 12. REPORT DATE<br>July 1991<br>13. NUMBER OF PAGES<br>46 |
| 14. MONITORING AGENCY NAME & ADDRESS *(if different from Controlling Office)* | | 15 SECURITY CLASS. *(of this report)*<br>Unclassified<br>15a. DECLASSIFICATION/DOWNGRADING SCHEDULE |

16. DISTRIBUTION STATEMENT *(of this Report)*

Approved for public release; distribution unlimited.

17. DISTRIBUTION STATEMENT *(of the abstract entered in Block 20, if different from Report)*

18. SUPPLEMENTARY NOTES

*Presently at the U.S. Army Aviation Systems Command, St. Louis, MO 63120-1798.

19. KEY WORDS *(Continue on reverse side if necessary and identify by block number)*

| | | |
|---|---|---|
| Alloy steels | Corrosion | Hydrogen embrittlement |
| 4340 steels | Fatigue | |
| High strength steels | Stress corrosion cracking | |

20. ABSTRACT *(Continue on reverse side if necessary and identify by block number)*

(SEE REVERSE SIDE)

DD FORM 1 JAN 73 1473 EDITION OF 1 NOV 65 IS OBSOLETE

UNCLASSIFIED

SECURITY CLASSIFICATION OF THIS PAGE *(When Data Entered)*

Block No. 20

ABSTRACT

The U.S. Army Materials Technology Laboratory (MTL) conducted a failure analysis of a mixer pivot support located on the AH-64 Apache Helicopter. The component was found to be broken in two pieces during an inspection in Saudi Arabia while the aircraft was being utilized for Operation Desert Storm.

Visual inspection of the failed part revealed significant wear on surfaces that contacted the bushing and areas at the machined radius where the cadmium coating had been damaged allowing corrosion pitting to occur. Light optical microscopy showed that the crack origin was located at the machined radius within a region that was severely pitted. Metallographic examination of a cross section taken through the crack initiation site revealed cracks at the bottom of some pits running parallel to the fracture plane. The hardness, chemistry, and microstructure of the electroslag remelted (ESR) 4340 steel used to fabricate the component conformed to required specifications and no apparent manufacturing defects were found. Electron microscopy showed that most of the fracture surface failed in an intergranular fashion with the exception of a shear lip zone which exhibited a dimpled morphology. The failure was set into action by hydrogen charging as a result of corrosion and was aggravated by the stress concentration effects of pitting at the radius and the high notch sensitivity of the material. Energy dispersive spectroscopy (EDS) determined that deposits of sand, corrosion, and salts were found within the pits. The failure mechanism was hydrogen assisted and was most likely a combination of stress corrosion cracking and corrosion fatigue. Recommendations have been made to improve the inspection criteria of the component in service and the material utilized in fabrication.

## CONTENTS


Page

BACKGROUND . . . . . 1

VISUAL INSPECTION AND LIGHT MICROSCOPY . . . . . 1

METALLOGRAPHIC EXAMINATION . . . . . 2

TENSILE TESTING . . . . . 3

HARDNESS TESTING . . . . . 3

CHEMICAL ANALYSIS . . . . . 4

ELECTRON MICROSCOPY . . . . . 5

CONCLUSIONS

- Crack Initiation . . . . . 5
- Corrosion Pitting . . . . . 6
- Materials Characterization ESR 4340 Steel . . . . . 6
- Mode of Failure . . . . . 6
- Failure Scenario . . . . . 6
- Failure Mechanism . . . . . 6

RECOMMENDATIONS . . . . . 6

ACKNOWLEDGMENTS . . . . . 7

## BACKGROUND

The U.S. Army Materials Technology Laboratory (MTL) was requested by the Army Aviation Systems Command (AVSCOM) to conduct a metallurgical examination of a mixer pivot support, PN 7-211160043 SN 0525, which had failed in Saudi Arabia on an AH-64 Apache Helicopter. The mixer pivot support is a flight safety, critical component and is part of the rotor support assembly as shown in Figure 1. The mixer pivot support fits through the transmission support. Upon inspection on January 11, 1991, the component was found to be broken in half after being in service for approximately 1449 days (according to a category I deficiency report filed by SSG Daniel Swanson). The original replacement time for the mixer pivot support, as recommended by AVSCOM, was 800 days. However, the 800 day service life limitation had been extended to 1440 days due to a lack of available spare parts. A second extension was granted by AVSCOM for the same reason and the component was allowed to remain in service for up to 6 months beyond 1440 days as long as no corrosion was observed on the surface upon inspection. The mixer pivot support was machined from 4340 steel bar stock and hardened to HRC 54-57 as designated on McDonnell-Douglas engineering drawing number 7-211160043. The component was subsequently cadmium coated by a vacuum deposition process.

## VISUAL INSPECTION AND LIGHT OPTICAL MICROSCOPY

Figure 2 is a schematic of the mixer pivot support, showing the location of the failure. The failure site had been previously analyzed for stress concentrations by McDonnell-Douglas and was not identified as the most critical area. Other regions on the part were calculated as having higher stress concentrations (Kt values). Figure 3 shows the broken component in the as-received condition. Figure 4 was photographed after rotating the mixer pivot support 180°. The upper half (Part A) of the component which contained the bearing was in relatively good condition, as compared to the lower half (Part B). The surface coating of Part A was intact and the serial numbers and manufacturing identification data were easily distinguishable. There were no obvious signs of corrosion or mechanical damage to Part A. In contrast, however, Part B showed significant wear on surfaces that contacted the bushing. These regions are characterized by dark stains (designated by the arrows) in the macrograph. The cadmium coating appeared to have been almost entirely worn away during service and severe corrosion pitting had occurred in these areas.

Figure 5 is a graphic example of an area approximately 1.5 cm away from the major fracture, but within the fretted region, showing deep pits on the surface of Part B. A few of the pits were large and shallow and may have been formed to some extent by mechanical vibration in addition to corrosion. Deposits of corrosion products and other debris were found in clumps surrounding and filling a number of the pits. Figure 6 reveals a crack at the bottom of one pit. Note the roughened surface and extensive corrosion. Figure 7 shows another pit at higher magnification. In this instance, an interconnecting series of cracks were observed in the corrosion layer at the bottom of the pit. It was uncertain from visual inspection whether the cracks extended into the base material. However, metallographic examination performed later in the investigation of cross sections taken through these areas, revealed evidence of cracks originating from the bottom of pits and extending into the steel.

Figure 8A is a fractograph of Part A which was taken by exposing the fracture surface under a series of various light sources which were directed onto the macroscopic features at very acute angles. Normally, such a photograph consists of a single exposure but due to the

complexity and geometry of the fracture, four separate exposures were taken and subsequently blended together with light to obtain the contrast needed to reveal the important features of the fracture surface. Figure 8B is a schematic of fracture Face A which identifies the crack initiation site and traces the fracture path. The fracture plane intersected the radius at the crack origin. The radial lines and chevron patterns indicated that the fracture proceeded from the bottom right of the photograph (as designated by the arrow) up along both sides of the central hole. Where the two fractures meet at the top, a ridge is visible. This suggested that the fracture, indeed originated at the bottom radius, as illustrated.

Figure 9A is a fractograph of Part B which also reveals the crack origin and direction of propagation. The fracture face was badly smeared in many areas, as indicated by the bright spots on the photograph. This may have been caused by improper handling of the fractured component prior to examination, possibly the result of forcing both halves of the fracture faces together. Damage may have also occurred when the component was removed from the aircraft or after it had failed. In all cases the surface smearing is attributable to a post-fracture incident. An important feature of the fracture, located at the very top of the photograph, is a shear lip region where final fracture had occurred. Both Faces A and B contained surfaces that were very flat-faced in appearance, displaying no signs of plasticity, which is often associated with a brittle fracture. The shear lip zone, however, showed evidence of ductility. The existence of a shear lip zone served to further substantiate the location identified as the crack origin, since final fracture would tend to occur in an area opposite the initiation site on this component.

Extensive corrosion pitting was another critical feature found at the crack origin and adjacent to the fracture plane. Figure 10 shows this corrosion near the crack initiation site and on the radius (high stress concentration area) of fracture Face B. The corrosion is located just beyond the region of severe fretting, as identified in the photograph (see Figure 10). Figure 11 reveals this pitted region at higher magnification. The bright feature bordering the radius and fracture plane is smeared metal which is highly reflective. The pits were concentrated at the crack origin and were considered to be relatively deep (as confirmed later by metallographic examination) for this material in the hardened condition (HRC 54-57).

Figure 12 is a schematic which defines the area of fretting and its location relative to the fracture plane. It is important to note that the region of severe fretting was located just below the fracture plane and crack origin. Figure 13 is a macrograph of the crack initiation site located on fracture Face A. Again extensive corrosion pitting had occurred in this region. Figure 14 shows the corrosive attack at higher magnification. The entire area had experienced severe attack.

## METALLOGRAPHIC EXAMINATION

Figure 15A illustrates the areas where metallographic specimens were sectioned from Part B of the mixer pivot support. A ring of material was taken approximately 3/4 of an inch away from the fracture face. In addition to the longitudinal and transverse specimens sectioned from the ring, a third cross section was removed which contained extensive pitting on the exterior surface. Another cross section was taken through the crack origin of fracture Face B as shown schematically in Figure 15B. All of these specimens were utilized to characterize the microstructure of the material within specific areas of concern and to measure the depth of pitting.

Figures 16 and 17 are representative micrographs of the fine martensitic structure observed on all of the specimens examined. The microstructure was consistent with the heat treatment performed on the component. There was no evidence of unusual material defects or large inclusions. Figure 18 shows the cross section of the crack origin in the as-polished condition. The arrows in the photograph point out corrosion on the radius. Figure 19 reveals the same area in the etched condition. The only notable feature was banding which extends vertically in the micrograph and appears as alternating light and dark bands. Since the component was machined from ba- stock, the banding was the result of rolling during primary processing. The banding runs lengthwise to the mixer pivot support. Figure 20 represents the corrosion pits viewed in the top section of Figures 18 and 19. Note the cracks which originated from the bottom of these pits. The cracks extend parallel to the fracture plane. Figure 21 shows the same view as in Figure 20 but in the etched condition. The microstructure appeared uniform across the fracture plane and along the radius, with no signs of decarburization. The fold of metal located at the top of the micrograph surrounded by a dotted line on one side, represents an area that had been mechanically damaged after the fracture occurred and is of no significance to the cause of failure. Figure 22 shows the series of cracks identified by the arrow in Figure 21, at higher magnification. The cracks appear to extend in an intergranular fashion.

Figure 23 shows the pitted metallographic specimen in the as-polished condition. The large pit located in the center of the photograph has been magnified in Figure 24. The pit depth was approximately 18 mils. Figure 25 shows the same pit after the specimen was etched in a 1% Nital solution. Note the banding which extends horizontally across the photograph.

## TENSILE TESTING

The ring of material sectioned from Part B (as shown in Figure 15A), was subjected to tension testing. The specimen was C-shaped. Hardened bars were placed at the top and bottom of the C-ring specimen which was then fitted into the grips of a 20 Kip Instron Universal Electromechanical Tensile Test Machine. A crosshead speed of 0.05 inches per minute was utilized. The intent of this test was not to record the load and corresponding strain of the specimen until failure occurred, but simply to obtain fracture surfaces which could then be examined under the scanning electron microscope (SEM) and compared to the fracture under investigation.

Figure 26 is a macrograph of the two fracture faces of the C-ring specimen. The specimen displayed a ductile cup-cone fracture. Figure 27 represents the fracture morphology found over the entire area of the cup-cone surface. A dimpled topography was revealed, indicative of a ductile fracture mode.

## HARDNESS TESTING

A series of hardness measurements were performed circumferentially across a section of the C-ring specimen. Readings were taken on the concave surface of the ring as shown in Figure 28. The green coating located on this interior surface was removed with acetone prior to hardness testing. The required hardness of the component as sp ..fied on McDonnell-Douglas engineering drawing number 7-211160043 was HRC 54-57. The hardness results are listed in Table 1.

Table 1. MIXER PIVOT SUPPORT MACROHARDNESS MEASUREMENTS HRC SCALE 150 kg LOAD DIAMOND CONE PENETRATOR

| Reading | HRC |
|---|---|
| 1 | 56.0 |
| 2 | 55.5 |
| 3 | 56.0 |
| 4 | 55.0 |
| 5 | 56.0 |
| 6 | 55.5 |
| 7 | 55.5 |
| 8 | 56.0 |
| 9 | 55.5 |
| 10 | 55.0 |
| Average | 55.6 |
| Required | 54 - 57 |

## CHEMICAL ANALYSIS

The mixer pivot support was specified to be fabricated from electroslag remelted (ESR) 4340 steel bar stock according to the requirements contained in HMS-6-1121. Atomic absorption (AA) and inductively coupled argon plasma emission spectroscopy (ICP) were used to determine the chemical composition of the material. The carbon and sulfur content was analyzed by the LECO combustion method. The required compositional ranges for the material have been included for comparative purposes. The chemical composition of the material compares favorably as shown in Table 2.

Table 2. COMPARISON OF CHEMISTRIES

| Element | C | Mn | Si | P | S | Cr | Ni | Mo | Cu | Al | Fe |
|---|---|---|---|---|---|---|---|---|---|---|---|
| HMS-6-1121 | 0.39-0.41 | 0.60-0.80 | 0.20-0.35 | 0.010 MAX | 0.008 MAX | 0.70-0.90 | 1.65-2.00 | 0.20-0.30 | 0.35 MAX | 0.030 MAX | REMAIN |
| Mixed Pivot Support | 0.39 | 0.69 | 0.21 | 0.008 | 0.005 | 0.82 | 1.99 | 0.28 | 0.11 | 0.012 | REMAIN |

## ELECTRON MICROSCOPY

The fracture surfaces of the component were examined utilizing the SEM. Figure 29 is an SEM photograph of the crack initiation area located on fracture Face A. The fracture surface and corroded radius have been identified in the photograph. Extensive corrosion pitting was found along the edge identified as the crack origin, but as Figures 30 and 31 show, the exact point of crack initiation was difficult to resolve because of mechanical damage. Figures 30 and 31 represent area A of Figure 29. Note the smeared edges, as defined by the pairs of arrows in the SEM photograph, and the deep corrosion pits. Some of the pits were found to contain cracks, as revealed in Figure 32. Figure 33 was taken for comparative purposes and shows an area containing part of the fracture surface and the radius, where no corrosion was observed. A significant contrast in the condition of the surface finish of the radius can be seen when Figure 33 is placed alongside Figures 30 and 31. Corrosion did not occur at the radius viewed in Figure 33 because the protective cadmium plating was still intact. Figure 34 shows an SEM micrograph of the cadmium plating and the resulting energy dispersing spectroscopy (EDS) spectra obtained when the coating was analyzed. The major peaks of the EDS spectra were as anticipated. Cadmium was detected, representing the cadmium topcoat, and chromium was detected, most likely due to a final sealing procedure performed subsequent to the coating operation. A trace of silicon was also found and may be attributed to a number of various factors, including but not limited to surface greases, oils, or sand. Figure 35 shows an SEM micrograph taken within a pit and the chemical constituents in the region. The iron represents the base metal while cadmium represents the plating. Oxygen was also detected and is associated with an iron-oxide (corrosion product) or sand ($SiO_2$). A trace of calcium was found and could be representative of surface contamination due to handling. Silicon was detected in larger quantities. Close examination of surface particles revealed the presence of sand on fracture surfaces and within pits, as shown in Figure 36.

Figure 36 contains an SEM fractograph showing a sand particle (as denoted by the arrow) and the corresponding EDS analysis which consisted of silicon and oxygen with a trace of iron (from the base material). Figures 37 and 38 contain the EDS spectra obtained from the inside regions of other pits adjacent to the fracture. The most significant finding was the existence of chlorine which might be associated with salt water intrusion.

Figure 39 is an SEM fractograph of the typical morphology found on approximately 90% of the total fracture surface. The mode of failure that occurred from the crack origin up along both sides of the central hole experienced intergranular decohesion. The only area that fractured differently was within the shear lip region which displayed a predominantly dimpled topography as shown in Figure 40. No evidence of fatigue striations were observed but since these features are difficult to resolve in such high strength materials, fatigue could not be entirely ruled out as a failure mechanism.

## CONCLUSIONS

### Crack Initiation

The cracking of the mixer pivot support initiated at the machined radius within a region that was severely pitted. The fracture did not originate in a region where fretting was most severe.

### Corrosion Pitting

Deposits of sand, corrosion, and salts were found within the pits examined. The depths of some of the pits were as much as 18 mils. Metallographic examination of a cross section taken through the crack origin revealed cracks in the bottom of some pits. These cracks ran parallel to the fracture plane.

### Materials Characterization ESR 4340 Steel

The hardness, chemistry, and microstructure of the material conformed to the required specifications and no apparent manufacturing defects were found on the component.

### Mode of Failure

The fracture was brittle in nature; showing little ductility, with the exception of the shear lip region. The morphology of most of the entire fracture surface (approximately 90%) was intergranular while the shear lip region exhibited a predominantly ductile dimpled topography. When a section of material (C-ring) from the mixer pivot support was pulled to failure in tension, the resulting fracture morphology was primarily dimpled, indicative of a ductile failure.

### Failure Scenario

Severe corrosion pitting occurred along the machined radius of the component and served as a crack initiation site. Hydrogen diffused into the high strength material (HRC 56) as a result of the corrosion process and migrated into areas of high stress concentration (crack tip). Evidence substantiating this claim lies in the fact that when a section of material taken from the failed component was pulled to failure, the resulting fracture surface was dimpled but the failure mode over 90% of the fracture surface under investigation was intergranular. In addition, the final fracture region of the component (shear lip) also displayed a dimpled topography. Both serve as indicators that the material can fracture in a ductile fashion. It has been well documented that hydrogen assisted cracking occurs in an intergranular fashion in this type of material when heat treated to the hardened condition.

### Failure Mechanism

The failure was set into action due to hydrogen charging as a result of corrosion. This condition was aggravated by the stress concentration effects of pitting at the radius and the high notch sensitivity of the material. The failure mechanism was hydrogen assisted and was most likely a combination of stress cracking and corrosion fatigue.

## RECOMMENDATIONS

The pits that served as the crack initiation site occurred over an extended period (probably several months or longer) but definitely did not occur between the last inspection of the component and the time of the failure (9 days). Therefore, it is recommended that the component be removed from service at the first indication of corrosion. Visual inspection with the use of a magnifying lens can be used to detect corrosion in the field.

The component could continue to be utilized when hardened to HRC 54-57 if the above recommendation is strictly adhered to. In this way, the ballistic properties could be maintained. However, a more conservative approach, which would sacrifice some of the ballistic

properties of the material, would be to heat treat the component to a less hardened condition. This would decrease the notch sensitivity of the material and the inspection intervals could then be longer since the critical crack size would be increased.

## ACKNOWLEDGMENTS

The authors wish to extend their appreciation to Dr. John Beatty, Dr. David Broek, and Dr. Richard Sisson for their helpful discussions. In addition, the metallographic work of Mr. Andrew Zani and Mr. Jack Mullin along with the precision sectioning expertise of Mr. Leonard Bucciarelli are to be recognized.

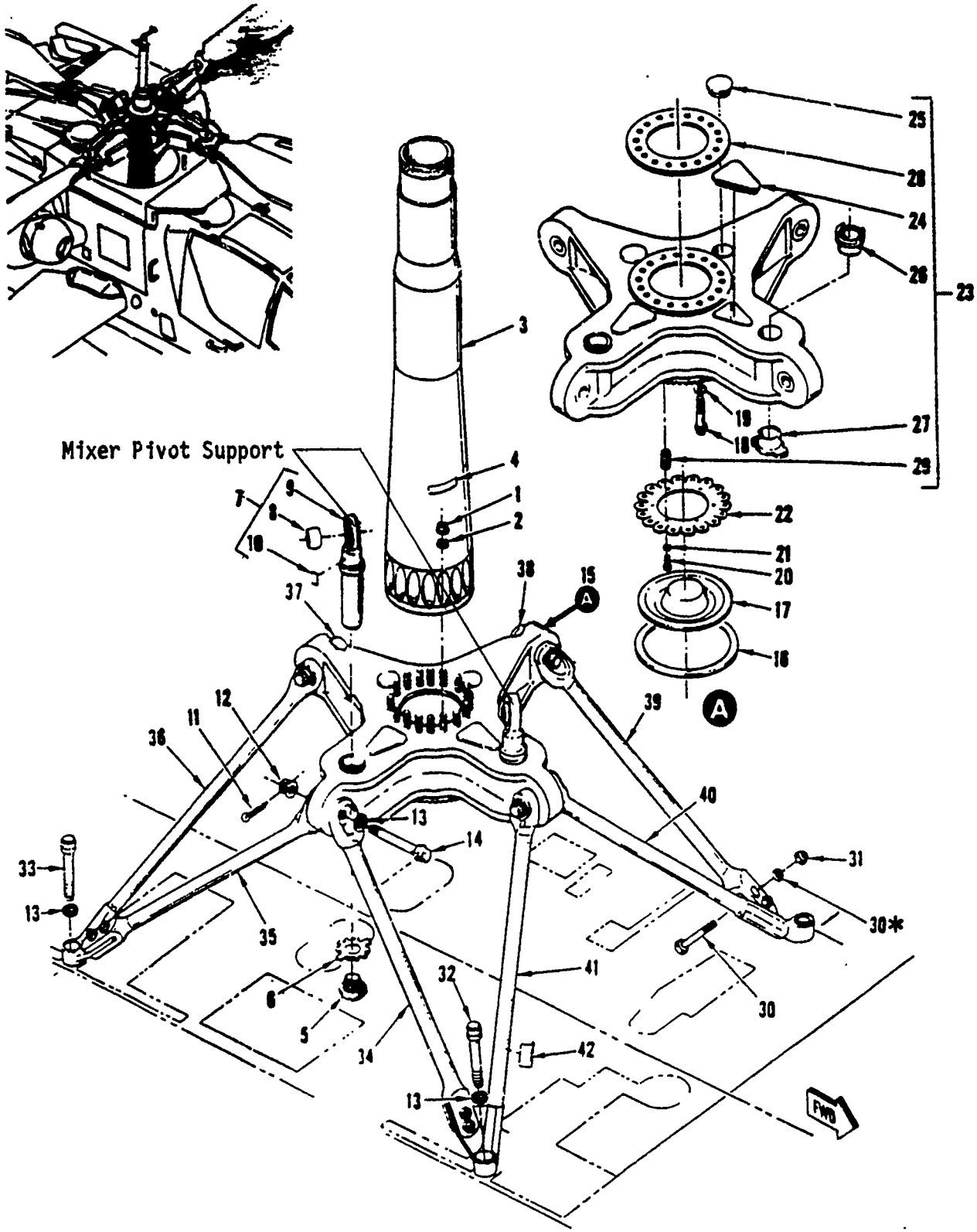


Figure 1. Schematic of the rotor support assembly. Mixer pivot support is item #9.

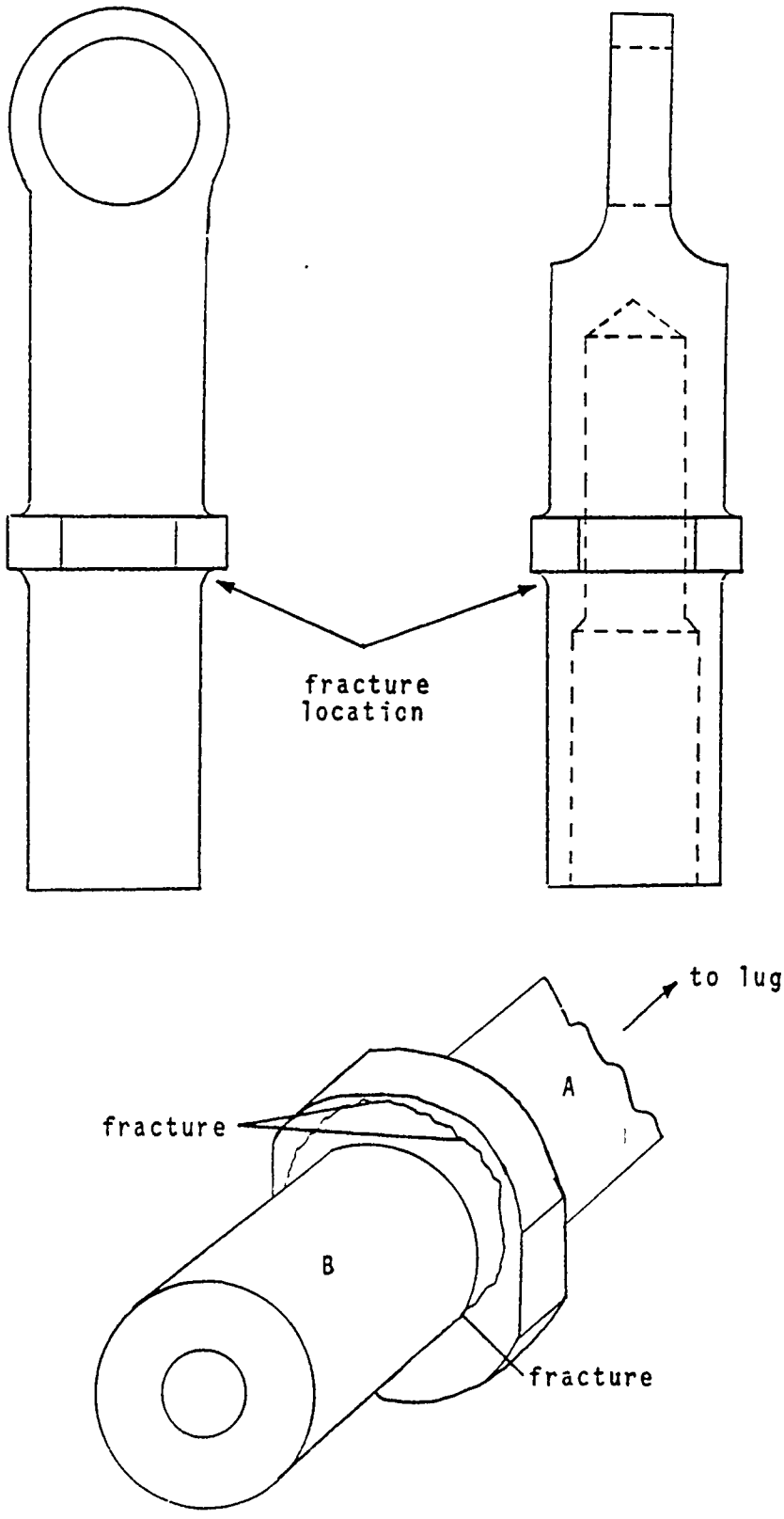


Figure 2. Schematic of mixer pivot support showing location of fracture.

**Part A**

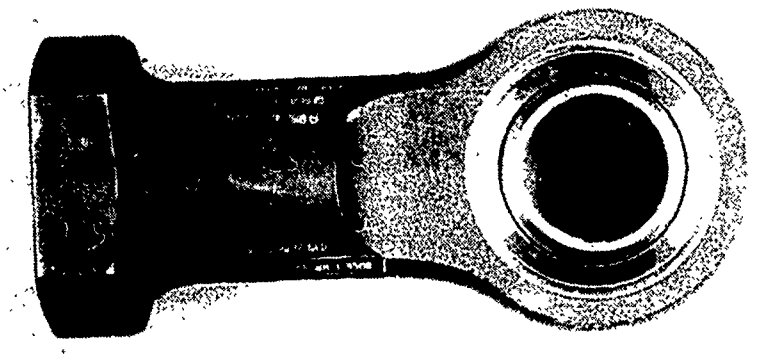

**Part B**

Figure 3. Shows the mixer support in the as-received condition.

## Part A

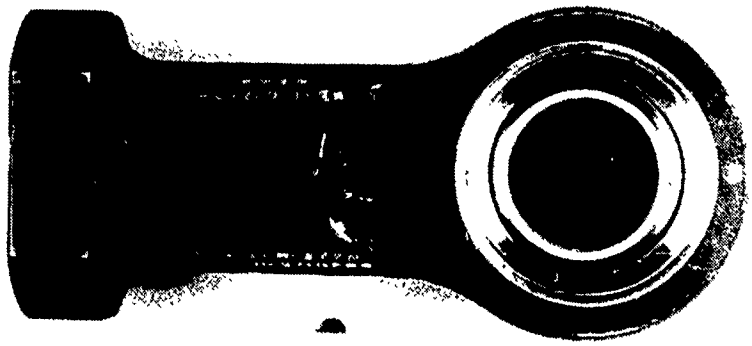

## Part B

Figure 4. Shows the part in the as-received condition rotated 180° from Figure 3.

Figure 5. Example of severe surface pitting. Mag. 7.5X.

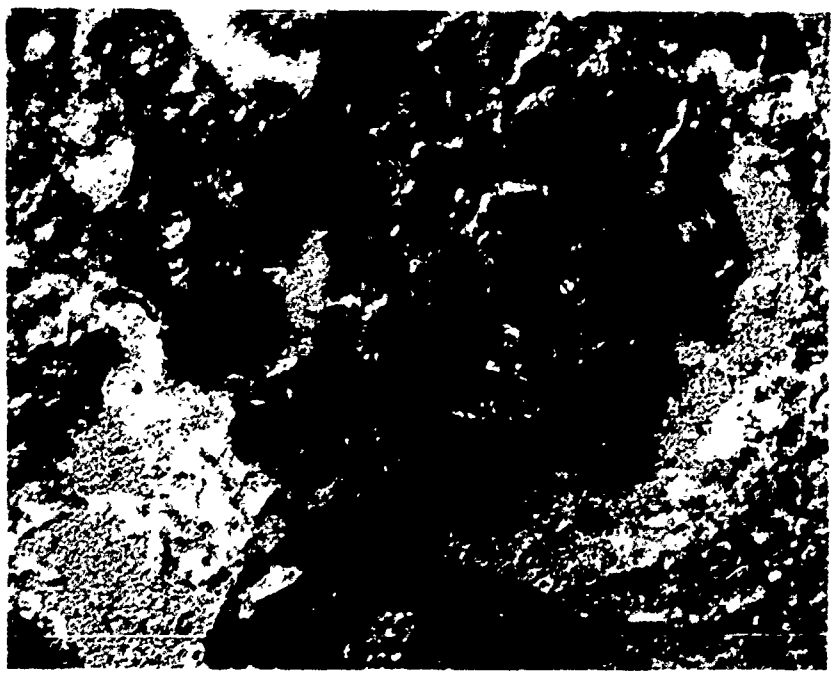

Figure 6. Cracking located at bottom of pit. Mag. 25X.

Figure 7. Shows cracking at the bottom of a pit. Mag. 50X.

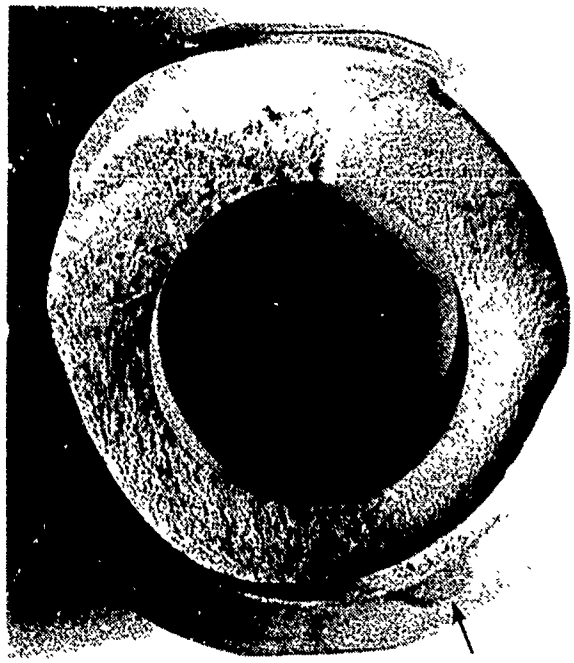

Figure 8A. Optical fractograph of Face A
(arrow identifies crack origin).

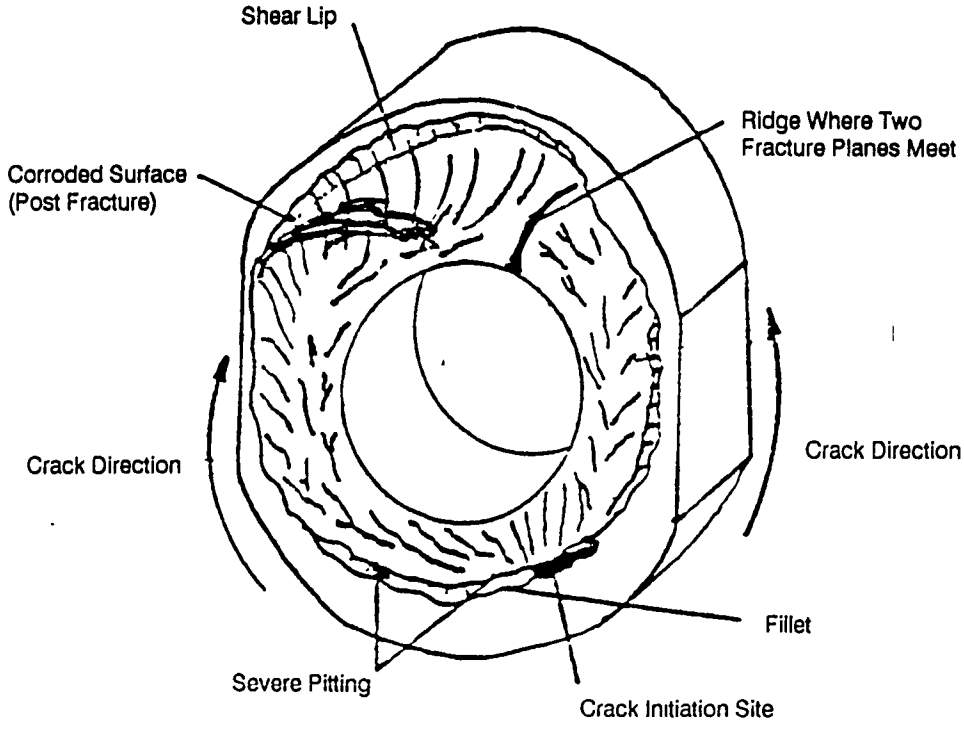


Figure 8B. Fracture Face A.

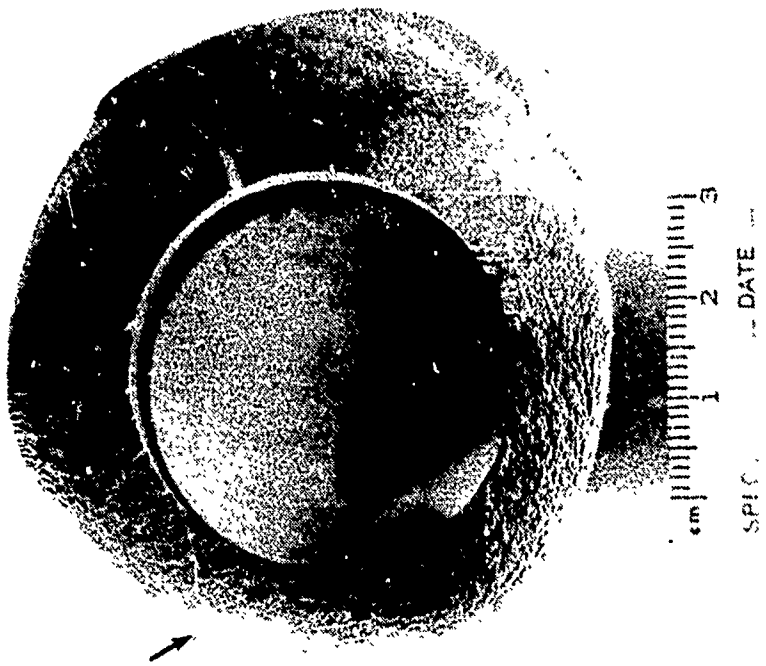

Figure 9A. Optical fractograph of Face B
(arrow identifies crack origin).

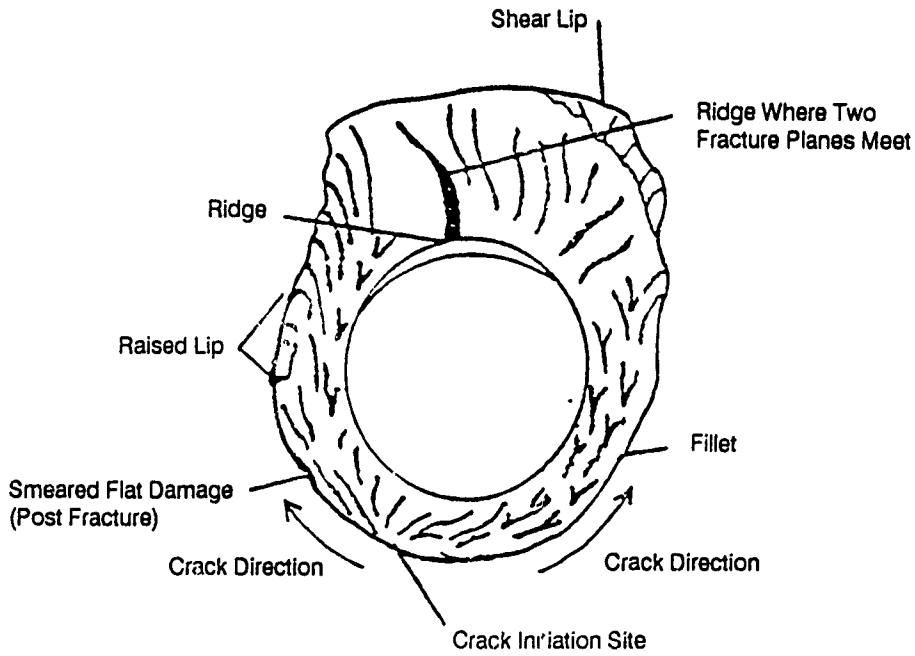


Figure 9B. Fracture Face B.

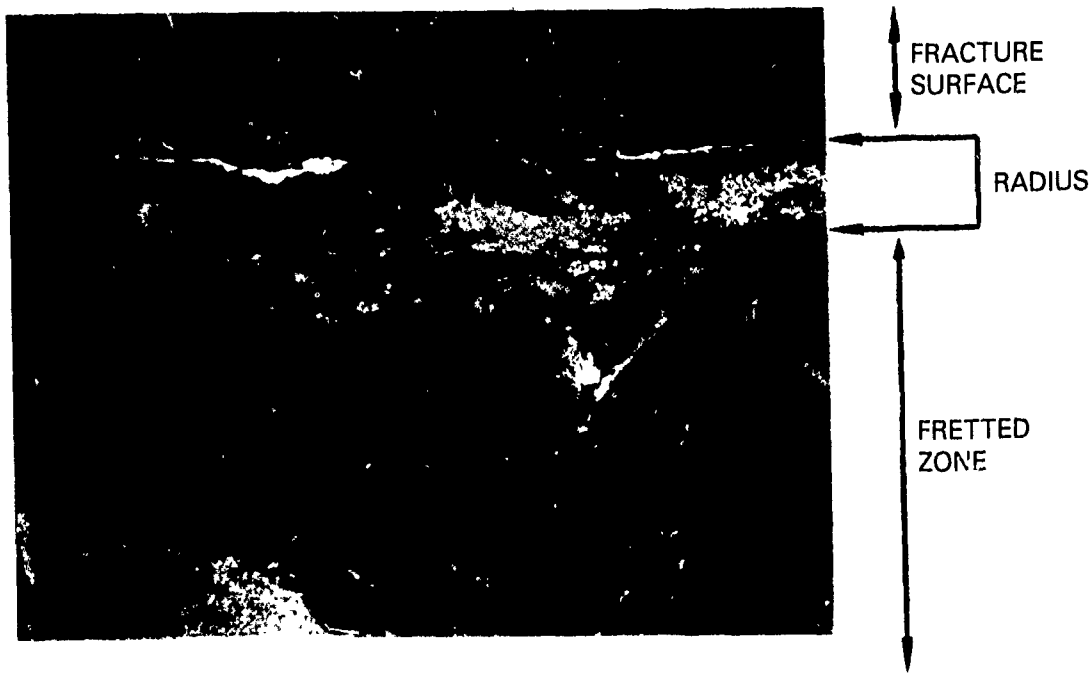


Figure 10. Crack initiation site of fracture Face B. Mag. 7.5X.

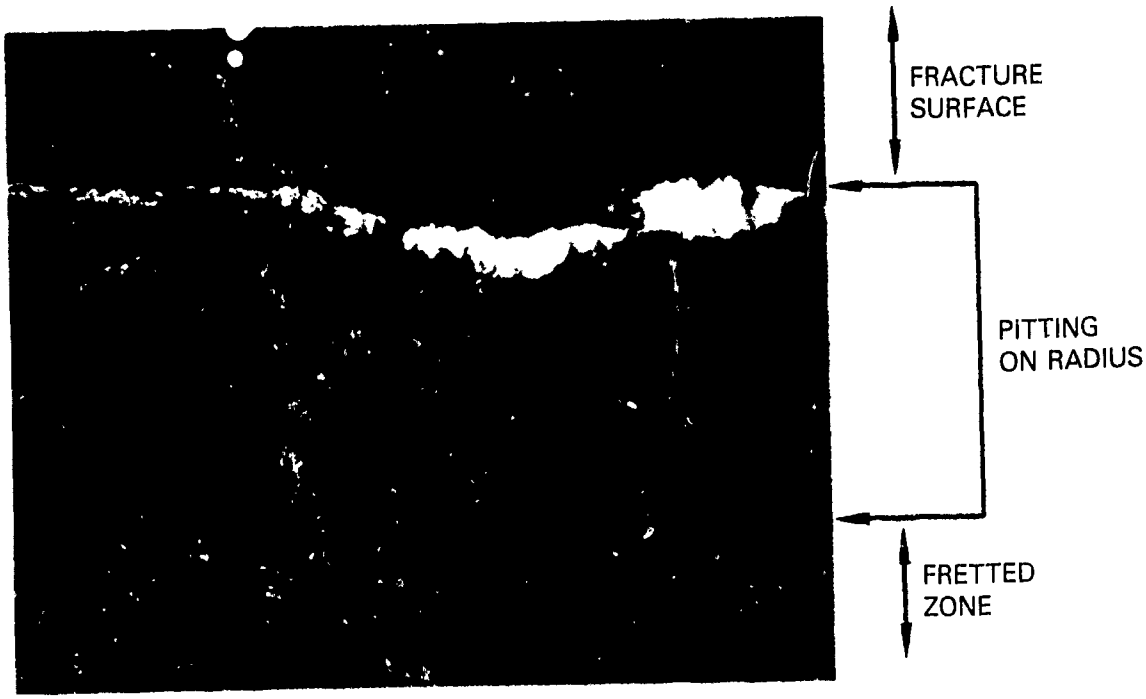


Figure 11. Corrosion pits at crack origin of fracture Face B. Mag. 30X.

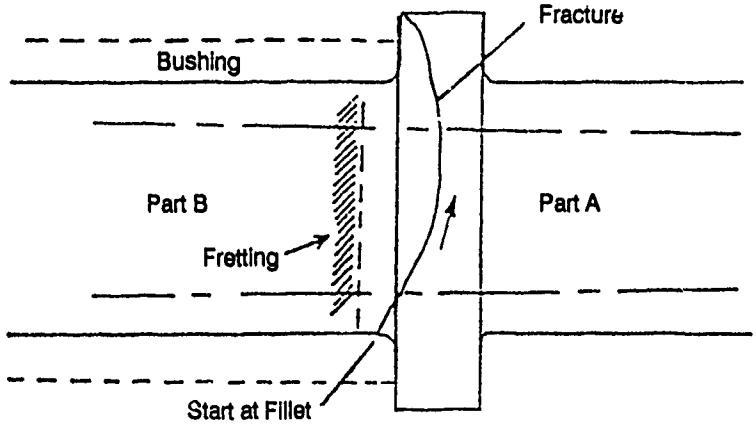


Figure 12. Schematic showing location of fracture and fretting.

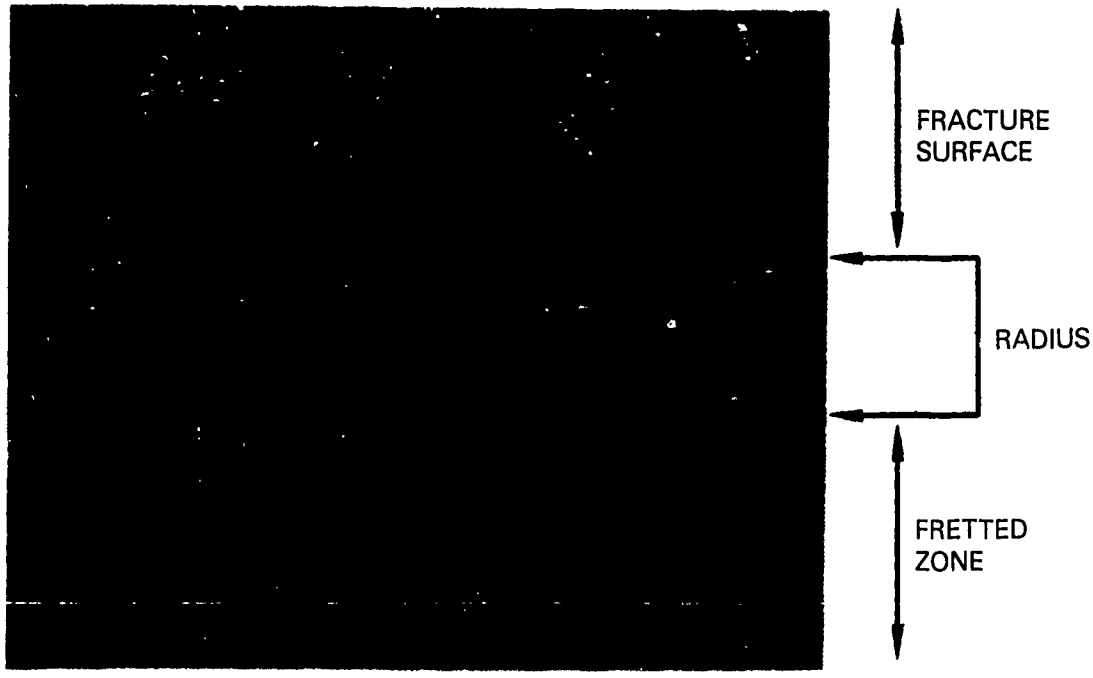


Figure 13. Crack initiation site of fracture Face A. Mag. 7.5X.

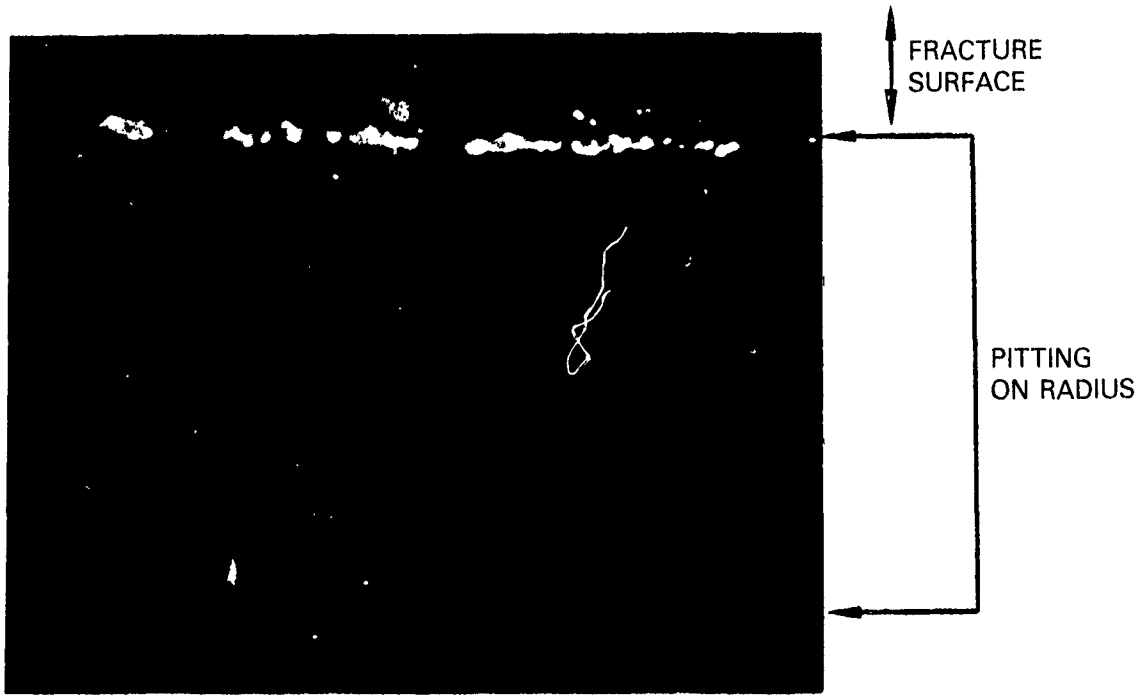


Figure 14. Corrosion pits at crack origin of fracture Face A. Mag. 30X.

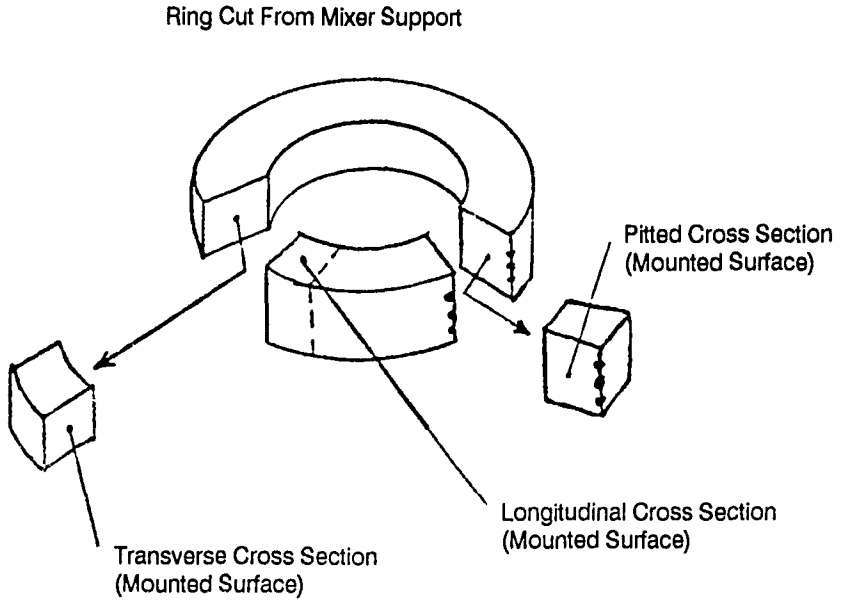


Figure 15A. Metallographic cross sections.

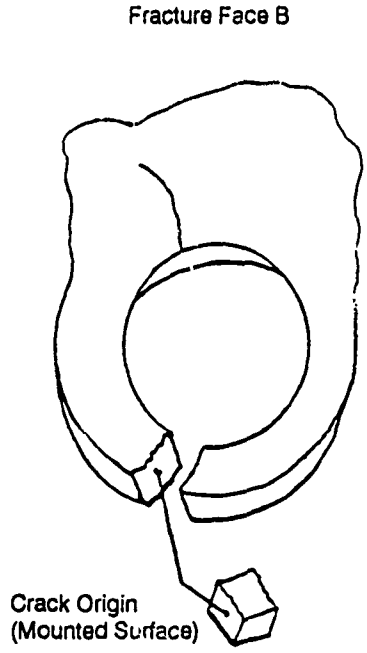


Figure 15B Metallographic cross sections.

Figure 16. Optical micrograph revealing a fine martensitic structure. Mag. 500X.

Figure 17. Shows fine tempered martensite indicative of prior heat treatment. Mag. 1000X.

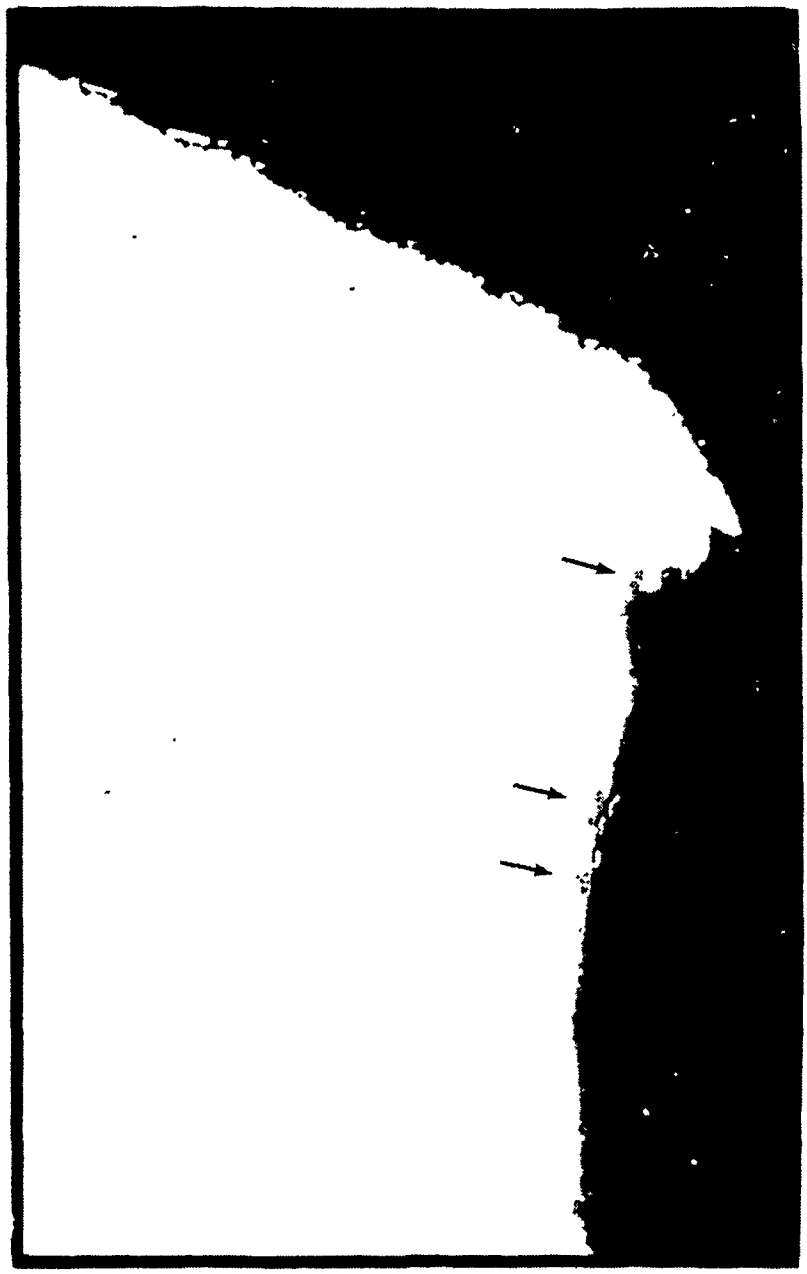

Figure 18. Cross section of crack origin taken through fracture Face B, in the as-polished condition. Mag. 50X.

Figure 19. Cross section of crack origin taken through fracture Face B, in the etched condition. Mag. 50X.

Figure 20. Corrosion pits with cracks as viewed on the top of Figures 18 and 19. Mag. 500X.

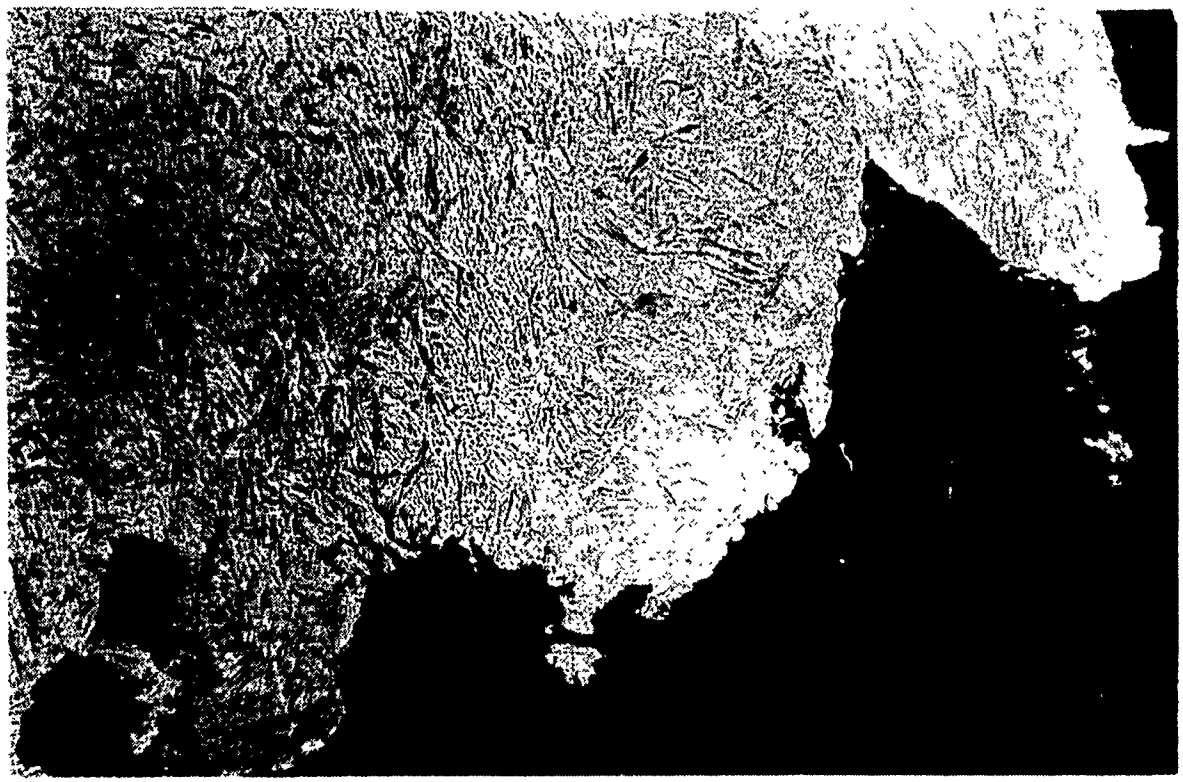

Figure 21. Same area as shown in Figure 20 after etching. Mag. 1500X.

Figure 22. Enlarged view of a crack at the bottom of a pit. Mag. 1500X.

Figure 23. Shows pitted cross section, refer to Figure 15A for location. Mag. 10X.

Figure 24. Shows large pit as seen in center of Figure 23. (Pit depth ~ 18 mils). Mag. 50X.

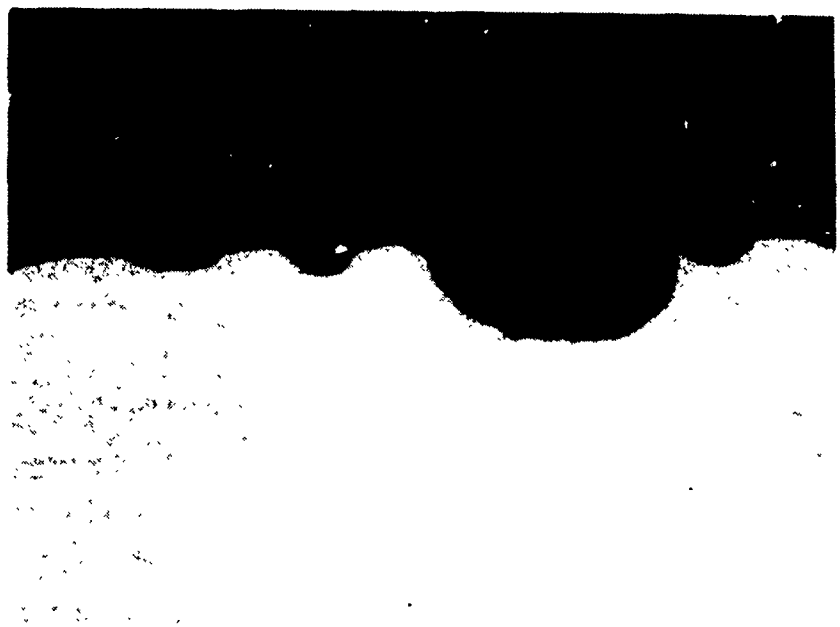

Figure 25. Shows pitted cross section after etching.
Note evidence of banding. Mag. 25X.

Figure 26. Fracture faces of the C-ring specimen. Mag. 2X.

Figure 27. Dimpled topography of fractured C-ring specimen. Mag. 1500X.

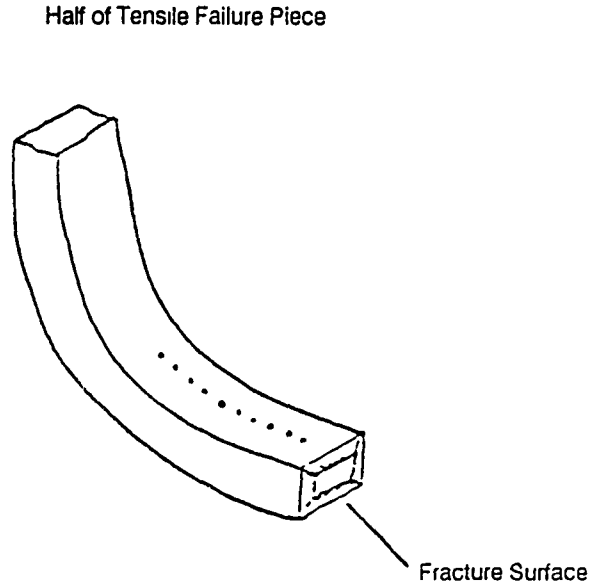


Figure 28. Hardness measurement locations.

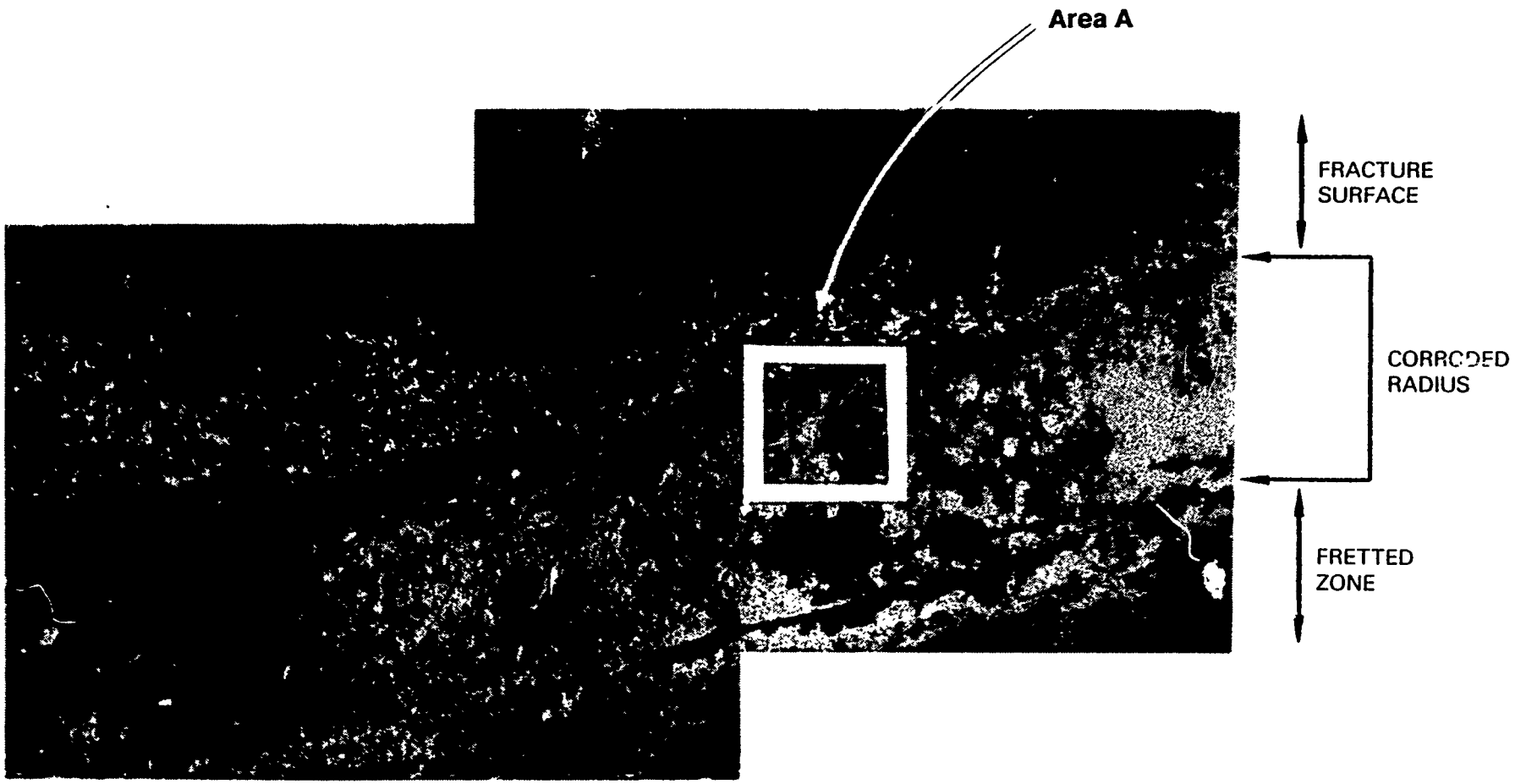


Figure 29. SEM of crack origin of fracture Face A. Mag. 13X.

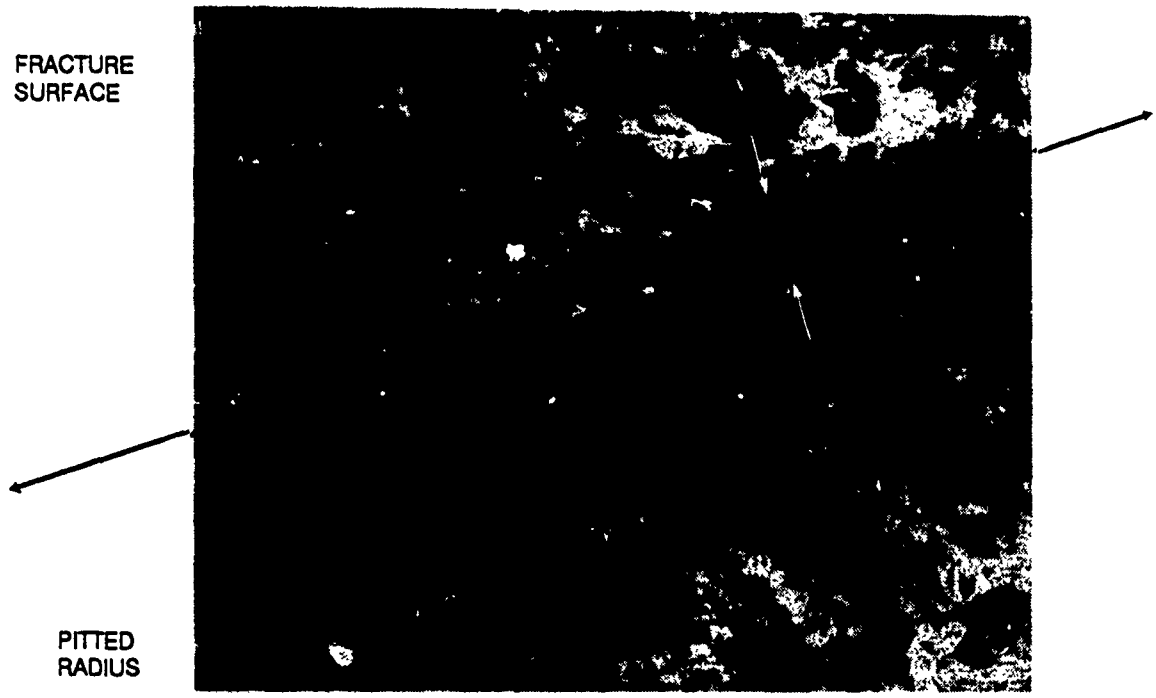


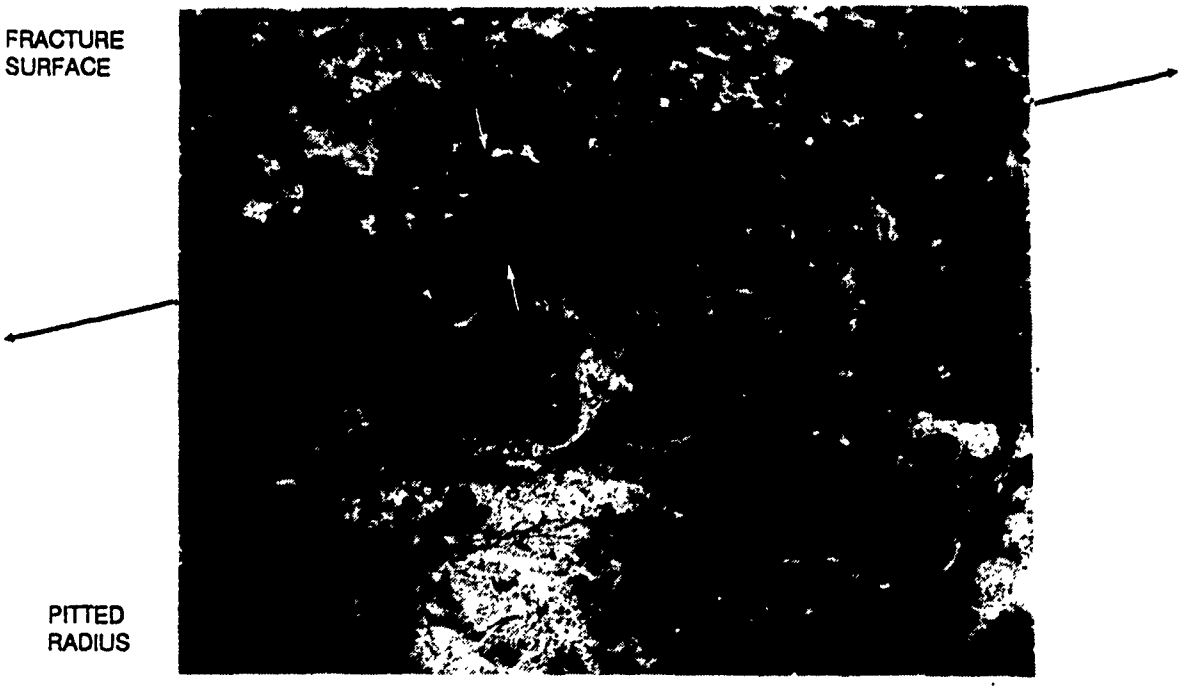


Figures 30 and 31. SEM of pits along radius a. crack origin. Mag. 75X.

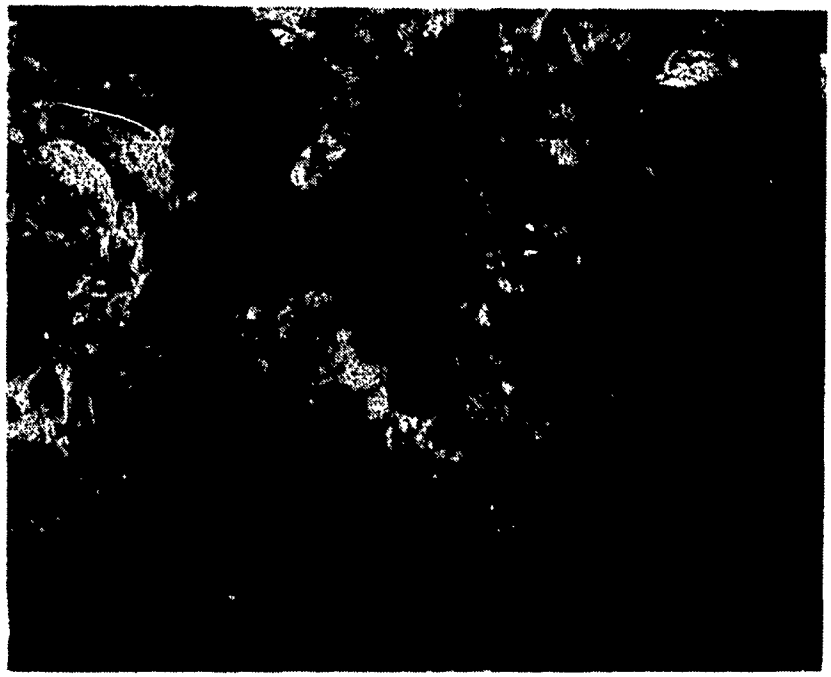

Figure 32. SEM of pits and secondary cracking. Mag. 130X.

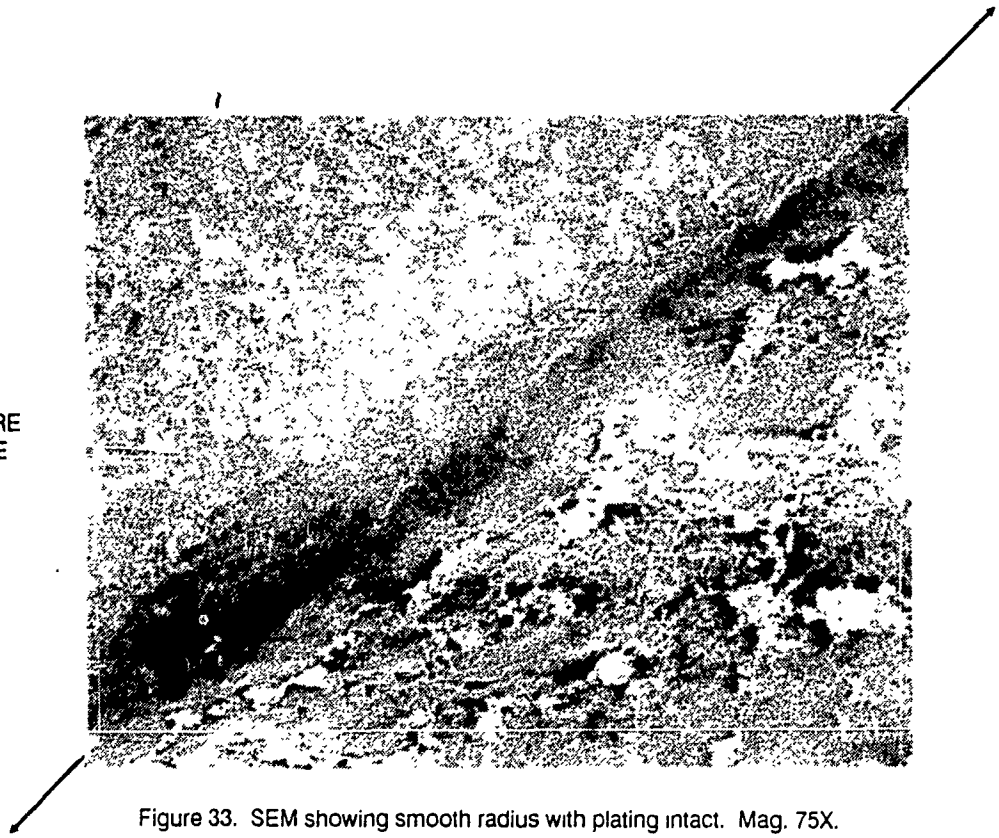


Figure 33. SEM showing smooth radius with plating intact. Mag. 75X.

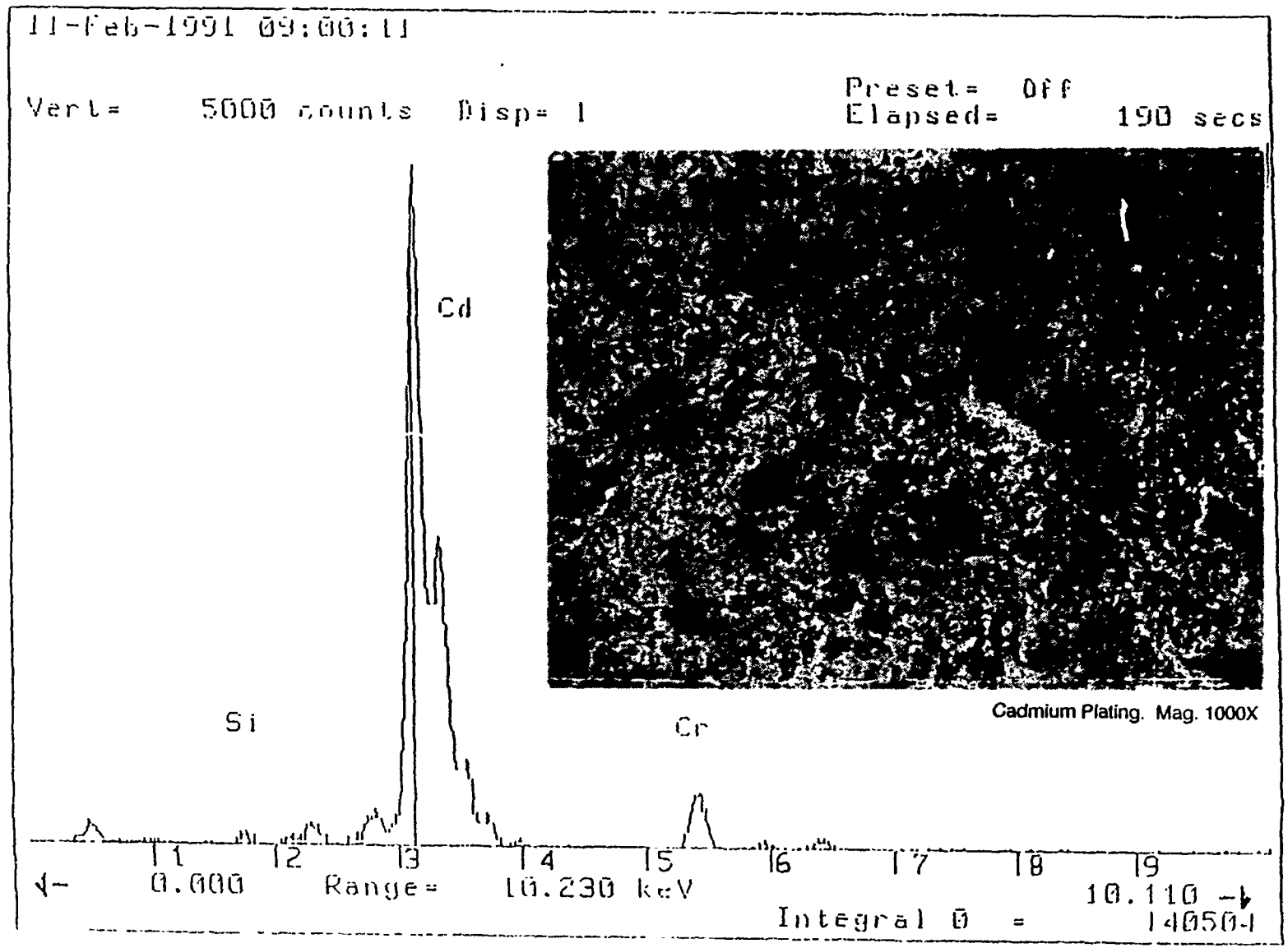


Figure 34 EDS spectra obtained from cadmium plating on radius.

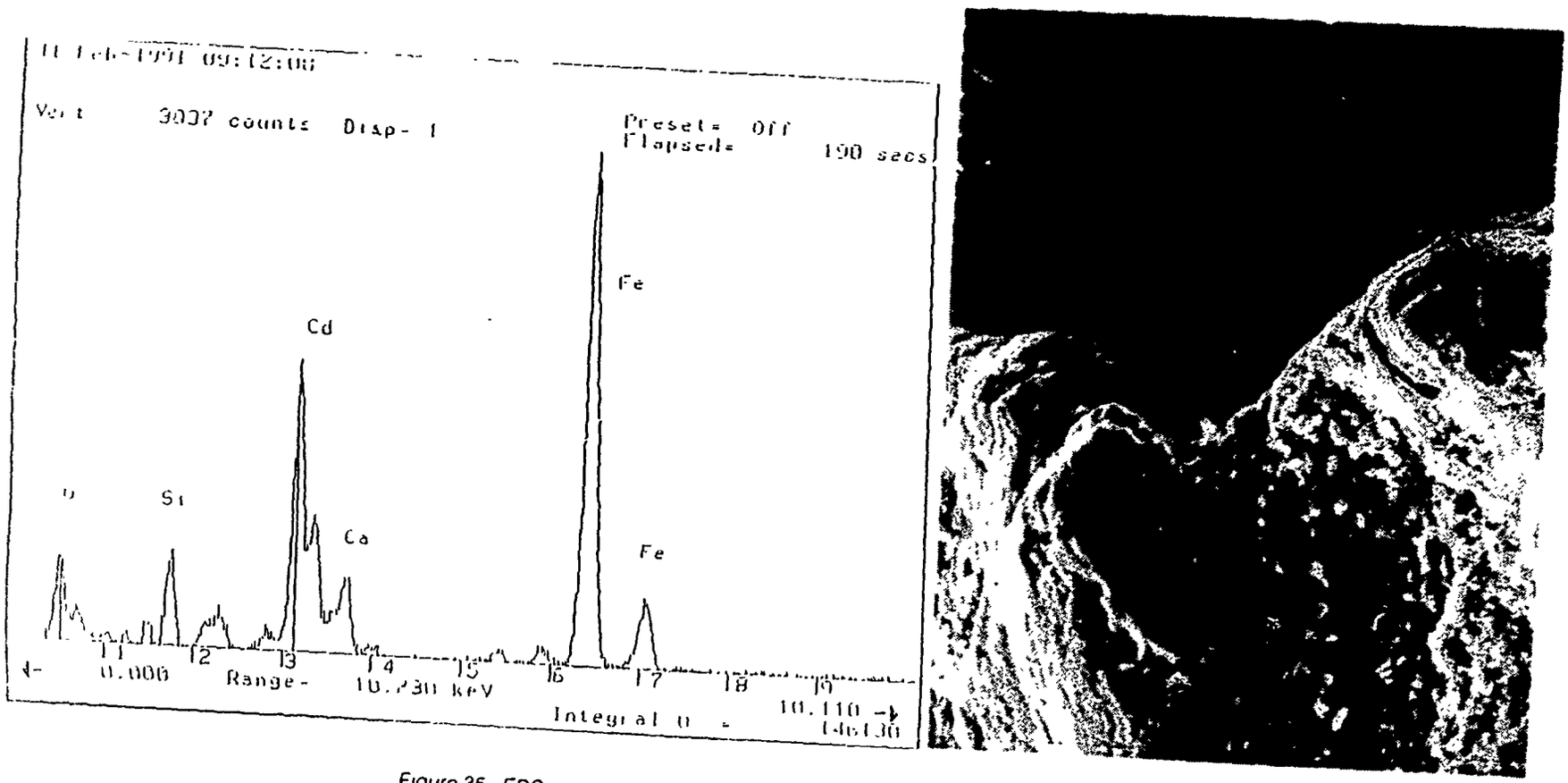


Figure 35. EDS spectra revealing chemical constituents within a pit.

Pitting. Mag 1000X

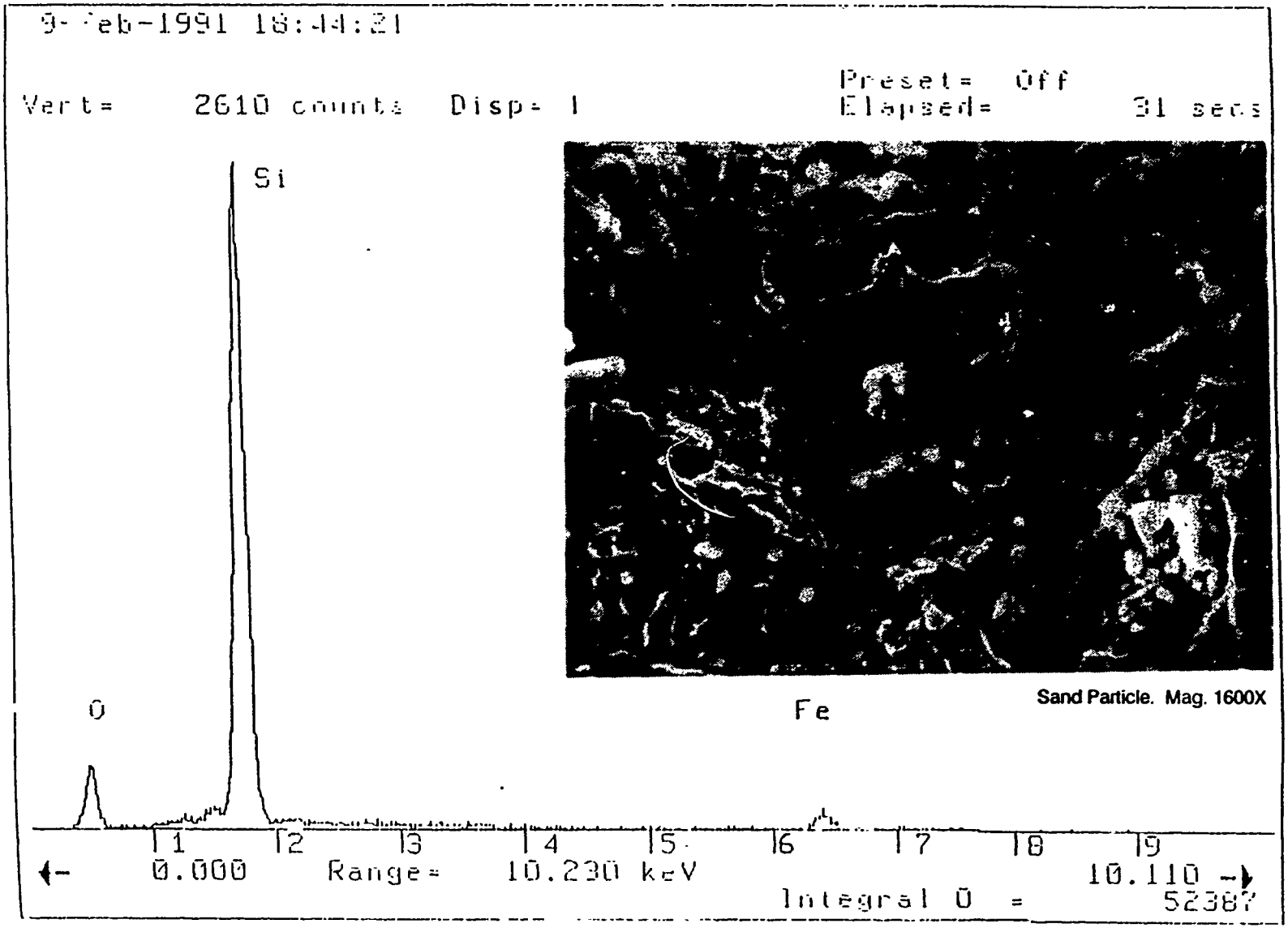


Figure 36. EDS spectra of a sand particle on fracture surface.

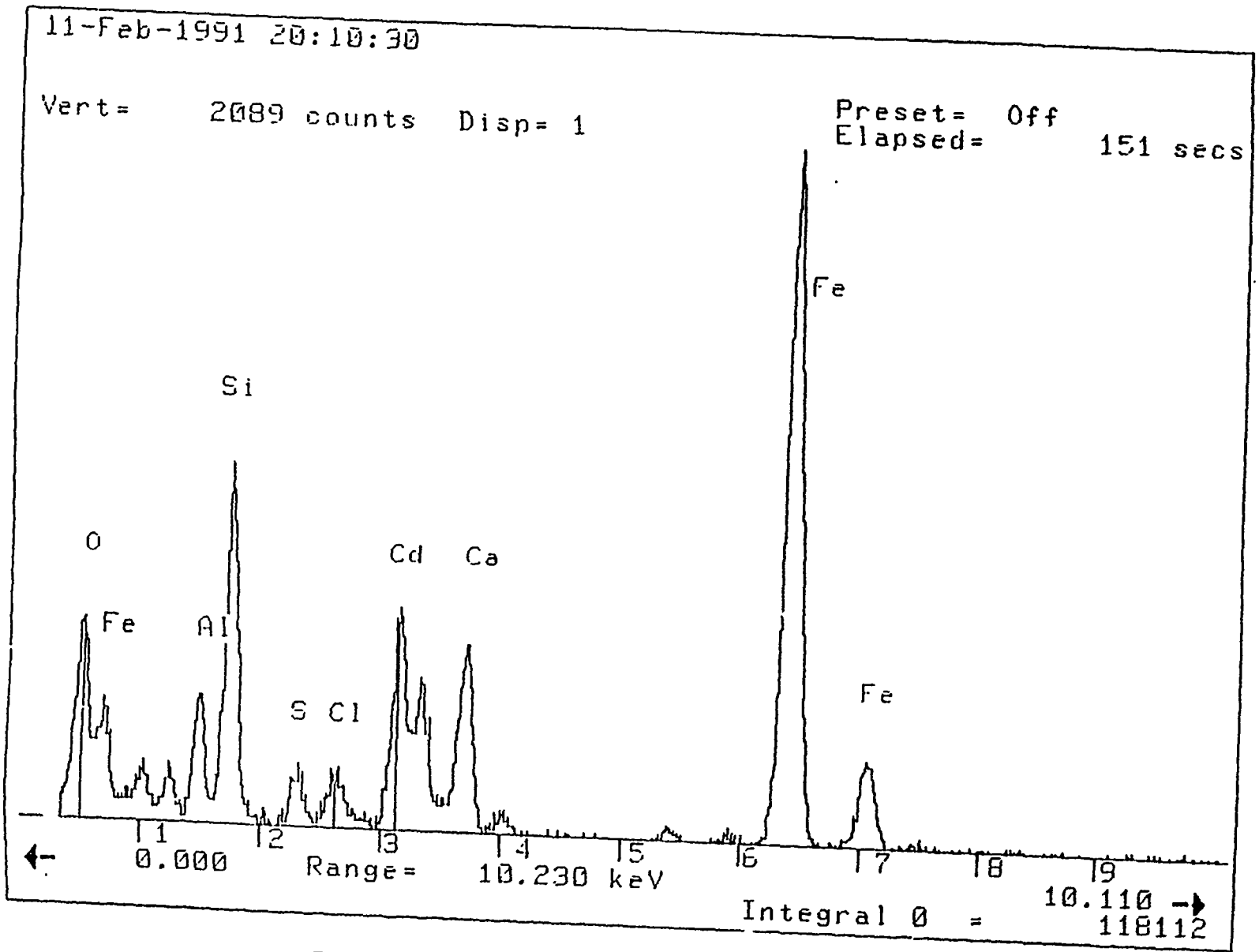


Figure 37. EDS spectra from within a pit adjacent to fracture.

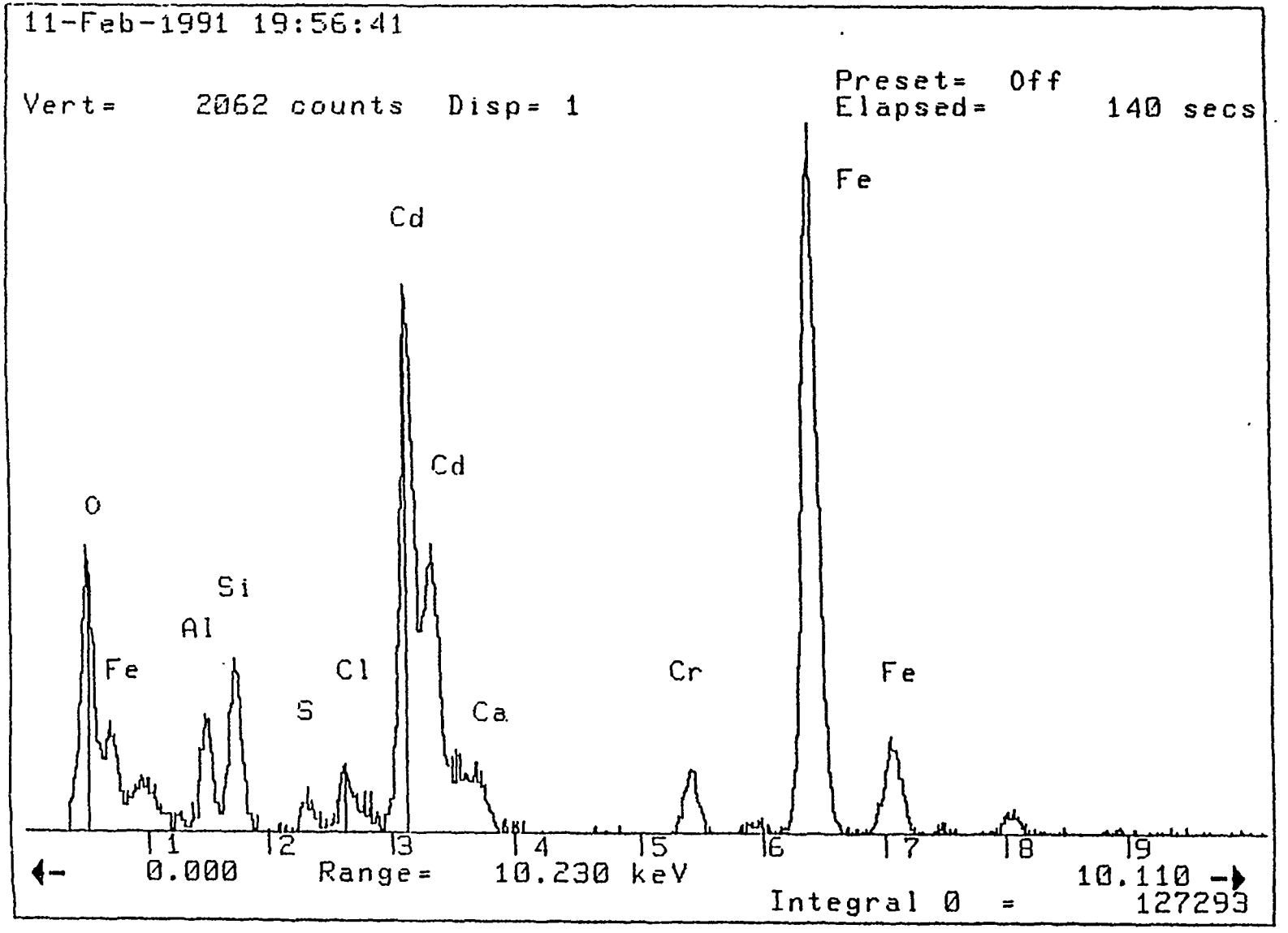


Figure 38. EDS spectra from within a pit adjacent to fracture.

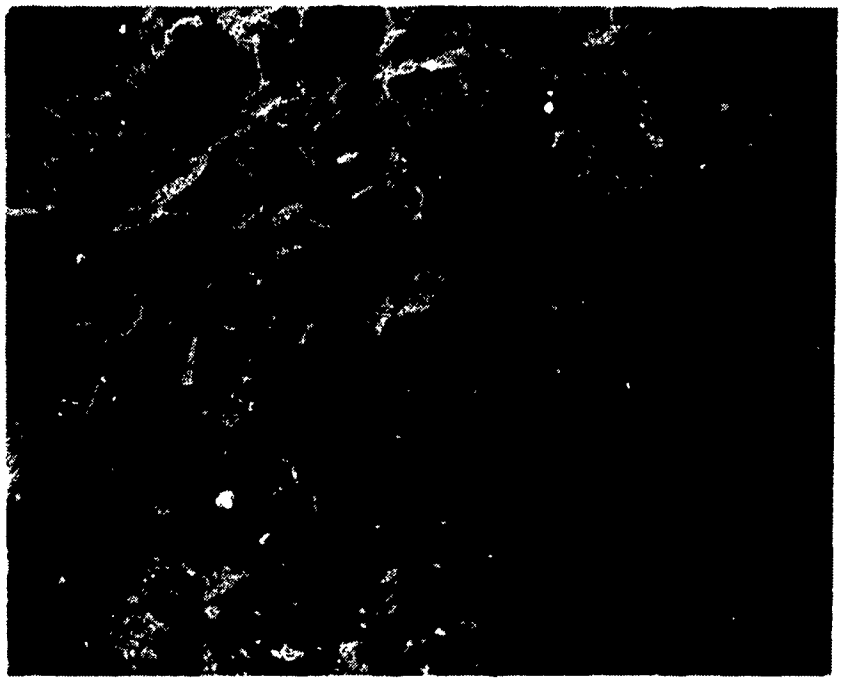

Figure 39. SEM showing intergranular mode of failure. Mag. 500X.

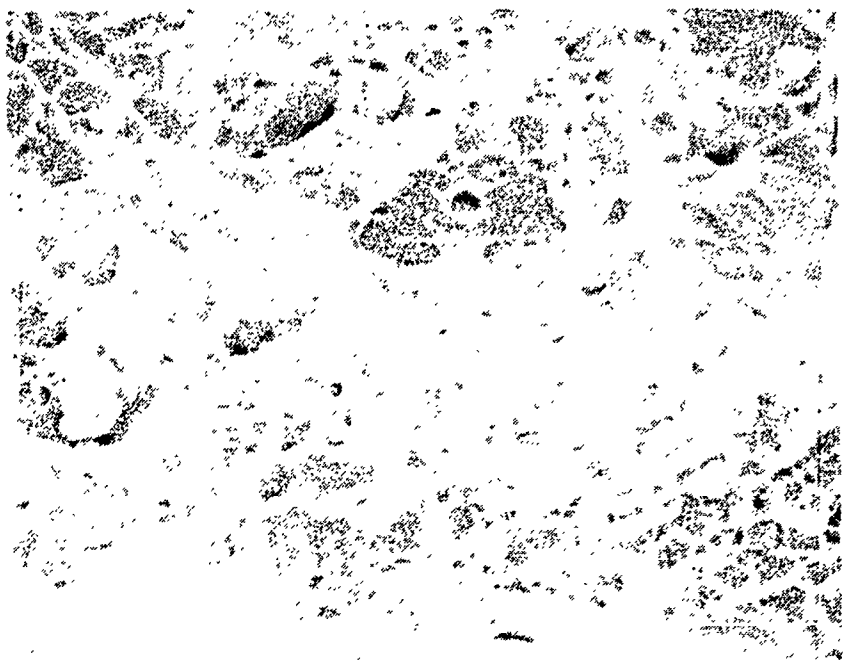

Figure 40. SEM showing a dimpled/quasi-cleavage fracture.
Mag. 2500X.

DISTRIBUTION LIST

| No. of Copies | To |
|---|---|
| 1 | Office of the Under Secretary of Defense for Research and Engineering, The Pentagon, Washington, DC 20301 |
| | Commander, Defense Technical Information Center, Cameron Station, Bldg. 5, 5010 Duke Street, Alexandria VA 22304-6145 |
| 2 | ATTN: DTIC-FDAC |
| 1 | MIAC/CINDAS, Purdue University, 2595 Yeager Road, West Lafayette, IN 47905 |
| | Commander, U.S. Army Materiel Command, 5001 Eisenhower Avenue, Alexandria, VA 22333 |
| 1 | ATTN: AMCSCI |
| 1 | AMCQA-P, S. J. Lorber |
| | Commander, Pacific Missile Test Center, Point Mugu, CA 93042 |
| 1 | ATTN: John Durda, Code 2041 |
| 1 | Carl Louck, Code 2041 |
| 1 | John Piercy, Code 2041 |
| 1 | Sam Keller, Code 2043 |
| 1 | Bill Mcauley, Code 2043 |
| | Commander, U.S. Army Laboratory Command, 2800 Powder Mill Road, Adelphi, MD 20783-1145 |
| 1 | ATTN: AMSLC-IM-TL |
| 1 | AMSLC-CT |
| | Commander, Rock Island Arsenal, Headquarters AMCCOM, Rock Island, IL 61299-6000 |
| 1 | ATTN: AMSMC-PCA-WM, Joe Wells |
| 1 | AMSMC-QAM-I, Gary Smith |
| 1 | AMSMC-ASR-M, Brian Kunkel |
| 1 | John Housseman |
| | Commander, U.S. Army Test and Evaluation Command, Aberdeen Proving Ground, MD 21005 |
| 1 | ATTN: Library |
| 1 | Clarke Engineer School Library, 3202 Nebraska Ave. North, Ft. Leonard Wood, MO 65473-5000 |
| | Naval Air System Command, Department of the Navy, Washington, DC 20360 |
| 1 | ATTN: AIR-03PAF |
| | Naval Research Laboratory, Washington, DC 20375 |
| 1 | ATTN: Code 5830 |
| | Naval Air Development Center, Warminster, PA 18974 |
| 1 | ATTN: Code 063 |
| | Commander, U.S. Army Aviation Systems Command (AVSCOM) St. Louis, MO 63120-1798 |
| 1 | ATTN: AMSAV-ECC, Emanuel Buelter |
| 1 | AMSAV-ECC, Robert Lawyer |
| 1 | AMSAV-EFM, Frank Barhorst |
| 1 | AMSAV-EFM, Kirit Bhansali |
| 1 | AMSAV-E, Carl Smith |
| 1 | AMCPM-AAH, Dave Roby |
| 1 | AMCPM-AAH, Bob Kennedy |
| | Commander, Corpus Christi Army Depot, Corpus Christi, TX 78419-6195 |
| 1 | ATTN: AMSAV-MRPD, Nicholas Hurta, Mail Stop 55 |
| 1 | AMSAV-MRPD, Lou Neri, Mail Stop 55 |
| 1 | SDSCC-QLM, David Garcia, Mail Stop 27 |
| 1 | SDSCC-QLM, Charlie Wilson, Mail Stop 27 |
| | Commander, Armament Research, Development and Engineering Center, Picatinny Arsenal, [illegible]7806-5000 |
| 1 | ATTN: SMCAR-CCS-C, Anthony Sebasto, Bldg. #1 |
| | Program Manager, Government-Industry Data Exchange, GIDEP Operations Center, Corona, CA 91720-2000 |
| 1 | ATTN: J. C. Richards, Program Director |
| | Director, U.S. Army Materials Technology Laboratory, Watertown, MA 02172-0001 |
| 2 | ATTN: SLCMT-TML |
| 4 | Authors |

U.S. Army Materials Technology Laboratory
Watertown, Massachusetts 02172-0001
FAILURE ANALYSIS OF THE APACHE MIXER PIVOT SUPPORT
Victor K. Champagne, Jr., Gary Wechsler, Marc S. Pepi and Kirit J. Bhansali

Technical Report MTL TR 91-25, July 1991, 46 pp- illus-tables:

AD_____
UNCLASSIFIED
UNLIMITED DISTRIBUTION

Key Words
Alloy steels
4340 steels
High strength steels

The U.S Army Materials Technology Laboratory (MTL) conducted a failure analysis of a mixer pivot support located on the AH-64 Apache Helicopter. The component was found to be broken in two pieces during an inspection in Saudi Arabia while the aircraft was being utilized for Operation Desert Storm. Visual inspection of the failed part revealed significant wear on surfaces that contacted the bushing and areas at the machined radius where the cadmium coating had been damaged allowing corrosion pitting to occur. Light optical microscopy showed that the crack origin was located at the machined radius within a region that was severely pitted. Metallographic examination of a cross section taken through the crack initiation site revealed cracks at the bottom of some pits running parallel to the fracture plane. The hardness, chemistry, and microstructure of the electroslag remelted (ESR) 4340 steel used to fabricate the component conformed to required specifications and no apparent manufacturing defects were found. Electron microscopy showed that most of the fracture surface failed in an intergranular fashion with the exception of a shear lip zone which exhibited a dimpled morphology. The failure was set into action by hydrogen charging as a result of corrosion and was aggravated by the stress concentration effects of pitting at the radius and the high notch sensitivity of the material. Energy dispersive spectroscopy (EDS) determined that deposits of sand, corrosion, and salts were found within the pits. The failure mechanism was hydrogen assisted and was most likely a combination of stress corrosion cracking and corrosion fatigue. Recommendations have been made to improve the inspection criteria of the component in service and the material utilized in fabrication.

U.S. Army Materials Technology Laboratory
Watertown, Massachusetts 02172-0001
FAILURE ANALYSIS OF THE APACHE MIXER PIVOT SUPPORT
Victor K. Champagne, Jr., Gary Wechsler, Marc S. Pepi and Kirit J. Bhansali

Technical Report MTL TR 91-25, July 1991, 46 pp- illus-tables:

AD_____
UNCLASSIFIED
UNLIMITED DISTRIBUTION

Key Words
Alloy steels
4340 steels
High strength steels

The U.S. Army Materials Technology Laboratory (MTL) conducted a failure analysis of a mixer pivot support located on the AH-64 Apache Helicopter. The component was found to be broken in two pieces during an inspection in Saudi Arabia while the aircraft was being utilized for Operation Desert Storm. Visual inspection of the failed part revealed significant wear on surfaces that contacted the bushing and areas at the machined radius where the cadmium coating had been damaged allowing corrosion pitting to occur. Light optical microscopy showed that the crack origin was located at the machined radius within a region that was severely pitted. Metallographic examination of a cross section taken through the crack initiation site revealed cracks at the bottom of some pits running parallel to the fracture plane. The hardness, chemistry, and microstructure of the electroslag remelted (ESR) 4340 steel used to fabricate the component conformed to required specifications and no apparent manufacturing defects were found. Electron microscopy showed that most of the fracture surface failed in an intergranular fashion with the exception of a shear lip zone which exhibited a dimpled morphology. The failure was set into action by hydrogen charging as a result of corrosion and was aggravated by the stress concentration effects of pitting at the radius and the high notch sensitivity of the material. Energy dispersive spectroscopy (EDS) determined that deposits of sand, corrosion, and salts were found within the pits. The failure mechanism was hydrogen assisted and was most likely a combination of stress corrosion cracking and corrosion fatigue. Recommendations have been made to improve the inspection criteria of the component in service and the material utilized in fabrication.

U S. Army Materials Technology Laboratory
Watertown, Massachusetts 02172-0001
FAILURE ANALYSIS OF THE APACHE MIXER PIVOT SUPPORT
Victor K. Champagne, Jr., Gary Wechsler, Marc S. Pepi and Kirit J Bhansali

Technical Report MTL TR 91-25, July 1991, 46 pp- illus-tables:

AD_____
UNCLASSIFIED
UNLIMITED DISTRIBUTION

Key Words
Alloy steels
4340 steels
High strength steels

The U S. Army Materials Techno gy Laboratory (MTL) conducted a failure analysis of a mixer pivot support located on the AH-64 Apache He copter. The component was found to be broken in two pieces during an inspection in Saudi Arabia while t e aircraft was being utilized for Operation Desert Storm. Visual inspection of the failed part revealed significant wear on surfaces that contacted the bushing and areas at the machined radius where the cadmium coating had been damaged allowing corrosion pitting to occur. Light optical microscopy showed that the crack origin was located at the machined radius within a region that was severely pitted. Metallographic examination of a cross section taken through the crack initiation site revealed cracks at the bottom of some pits running parallel to the fracture plane. The hardness, chemistry, and microstructure of the electroslag remelted (ESR) 4340 steel used to fabricate the component conformed to required specifications and no apparent manufacturing defects were found. Electron microscopy showed that most of the fracture surface failed in an intergranular fashion with the exception of a shear lip zone which exhibited a dimpled morphology. The failure was set into action by hydrogen charging as a result of corrosion and was aggravated by the stress concentration effects of pitting at the radius and the high notch sensitivity of the material. Energy dispersive spectroscopy (EDS) determined that deposits of sand, corrosion, and salts were found within the pits. The failure mechanism was hydrogen assisted and was most likely a combination of stress corrosion cracking and corrosion fatigue. Recommendations have been made to improve the inspection criteria of the component in service and the material utilized in fabrication.

U.S. Army Materials Technology Laboratory
Watertown, Massachusetts 02172-0001
FAILURE ANALYSIS OF THE APACHE MIXER PIVOT SUPPORT
Victor K. Champagne, Jr., Gary Wechsler, Marc S. Pepi and Kirit J. Bhansali

Technical Report MTL TR 91-25, July 1991, 46 pp- illus-tables:

AD_____
UNCLASSIFIED
UNLIMITED DISTRIBUTION

Key Words
Alloy steels
4340 steels
High strength steels

The U S. Army Materials Technology Laboratory (MTL) conducted a failure analysis of a mixer pivot support located on the AH-64 Apache Helicopter. The component was found to be broken in two pieces during an inspection in Saudi Arabia while the aircraft was being utilized for Operation Desert Storm. Visual inspection of the failed part revealed significant wear on surfaces that contacted the bushing and areas at the machined radius where the cadmium coating had been damaged allowing corrosion pitting to occur. Light optical microscopy showed that the crack origin was located at the machined radius within a region that was severely pitted. Metallographic examination of a cross section taken through the crack initiation site revealed cracks at the bottom of some pits running parallel to the fracture plane The hardness, chemistry, and microstructure of the electroslag remelted (ESR) 4340 steel used to fabricate the component conformed to required specifications and no apparent manufacturing defects were found. Electron microscopy showed that most of the fracture surface failed in an intergranular fashion with the exception of a shear lip zone which exhibited a dimpled morphology. The failure was set into action by hydrogen charging as a result of corrosion and was aggravated by the stress concentration effects of pitting at the radius and the high notch sensitivity of the material Energy dispersive spectroscopy (EDS) determined that deposits of sand, corrosion, and salts were found within the pits. The failure mechanism was hydrogen assisted and was most likely a combination of stress corrosion cracking and corrosion fatigue. Recommendations have been made to improve the inspection criteria of the component in service and the material utilized in fabrication.